

This is the accepted manuscript version of the contribution published as:

Op de Hipt, F., Diekkrüger, B., Steup, G., Yira, Y., Hoffmann, T., **Rode, M.** (2018):
Modeling the impact of climate change on water resources and soil erosion in a tropical
catchment in Burkina Faso, West Africa
Catena **163** , 63 – 77

The publisher's version is available at:

<http://dx.doi.org/10.1016/j.catena.2017.11.023>

Modeling the effect of land use and climate change on water resources and soil erosion in a tropical West African catchment (Dano, Burkina Faso) using SHETRAN

Felix Op de Hipt^{1*}, **Bernd Diekkrüger**¹, **Gero Steup**¹, **Yacouba Yira**¹, **Thomas Hoffmann**²,
Michael Rode³, **Kristian Näschen**¹

¹ Department of Geography, University of Bonn, Meckenheimer Allee 166, 53115 Bonn

² German Federal Institute of Hydrology, Am Mainzer Tor 1, 56068 Koblenz

³ Helmholtz Center for Environmental Research – UFZ, Brückstraße 3a, 39114 Magdeburg

* Corresponding author. Tel.: +49 2287360710; fax: +49 228736101. E-mail address: felixodh@uni-bonn.de (F. Op de Hipt).

1
2
3
4
5
6
7
8
9
10
11
12
13
14
15
16
17
18
19
20
21
22
23
24
25
26
27
28
29
30
31
32
33
34
35
36
37
38
39
40
41
42
43
44
45
46
47
48
49
50
51
52
53
54
55
56
57
58
59
60
61
62
63
64
65

1 Modeling the effect of land use and cli- 2 mate change on water resources and soil 3 erosion in a tropical West African catch- 4 ment (Dano, Burkina Faso) using 5 SHETRAN

6 Keywords: Hydrological modeling, Erosion modeling, Climate change, Land use change

7 **ABSTRACT**

8 This study investigates the effect of land use and land cover (LULC) and climate change on
9 catchment hydrology and soil erosion in the Dano catchment in south-western Burkina Faso
10 based on hydrological and soil erosion modeling. The past LULC change is studied using land
11 use maps of the years 1990, 2000, 2007 and 2013. Based on these maps future LULC scenari-
12 os were developed for the years 2019, 2025 and 2030. The observed past and modeled future
13 LULC are used to feed SHETRAN, a hydrological and soil erosion model. Observed and mod-
14 eled climate data cover the period 1990 – 2030.

15 The isolated influence of LULC change assuming a constant climate is simulated by applying the
16 seven LULC maps under observed climate data of the period 1990 – 2015. The isolated effect of
17 climate scenarios (RCP4.5 and 8.5 of CCLM4-8) is studied by applying the LULC map of 1990 to
18 the period 1990 – 2032. Additionally, we combined past modeled climate data and past ob-
19 served LULC maps. Two chronological and continuous simulations were used to estimate the
20 impact of LULC in the past and in the future by gradually applying the LULC maps. These simu-
21 lations consider the combined impact of LULC and climate change.

22 The simulations that assumed a constant climate and a changing LULC show increasing water
23 yield (3.6% – 46.5%) and mainly increasing specific sediment yield (-3.3% – 52.6%). The simula-

24 tions that assume constant LULC and climate as changing factor indicate increases in water
25 yield of 24.5% to 46.7% and in sediment yield of 31.1% to 54.7% between the periods 1990 –
26 2005 and 2006 - 2032. The continuous simulations signal a clear increase in water yield (20.3%
27 – 73.4%) and specific sediment yield (24.7% to 90.1%). Actual evapotranspiration is estimated
28 to change by between -7.3% (only LUCC) to +3.3% (only climate change). When comparing
29 observed LULC and climate change alone, climate change has a larger impact on discharge and
30 sediment yield, but LULC amplifies climate change impacts strongly. However, future LULC
31 (2019-2030) will have a stronger impact as currently observed.

32 **1 INTRODUCTION**

33 Population and economic growth are considered to be the most important drivers of land degra-
34 dation. Human-driven land use and land cover (LULC) changes influence water resources and
35 may intensify land degradation by water-related soil erosion and nutrient depletion (CILSS,
36 2016; UNEP, 2012). Especially in countries with fragile ecosystems, limited water and soil re-
37 sources, changes in the hydrological cycle through LULC and climate changes may lead to an
38 increased flood and drought risk as well as accelerated soil erosion rates. Understanding the
39 effect of LULC and climate change on water and soil resources is paramount especially in coun-
40 tries, such as Burkina Faso, whose societies are highly dependent on rain-fed agriculture.

41 The population in Burkina Faso is growing at annual rates of about 3% in the last decade (The
42 World Bank, 2017). The growing food demand and the expansion of settlement areas lead to
43 LULC change through the conversion of savanna vegetation to cropland and settlement area.
44 The increased pressure on soil resources reduce the agricultural production through nutrient
45 depletion and loss of fertile soil through soil erosion (CILSS, 2016). Assessing the long term im-
46 pact of LULC change on runoff generation and soil erosion is therefore important for decision
47 makers to plan environmental protection measures. However, the number of studies that investi-

48 gate feedback mechanisms between LULC change, runoff generation and soil erosion is limited
49 in West Africa.

50 Hydrological processes and soil erosion are closely linked and strongly controlled by LULC. Sus-
51 tainable management of water and soil resources require a combined consideration of water and
52 sediment fluxes (Diekkrüger, 2010). LULC change impacts can be studied by comparing field
53 measurements of hydrological and soil erosion variables from different LULC classes (Braithmoh
54 and Vlek, 2004; Giertz et al., 2010, 2005; Hiepe, 2008). Field measurements show that a change
55 from savanna or forest vegetation to cropland can reduce soil hydraulic conductivity and in-
56 creased surface runoff and soil erosion. This can be explained by the reduction of macroporosity
57 as result of decreased biological activity following the disturbance of the soil by agricultural activ-
58 ities (Giertz et al., 2005). However, measurement of soil erosion is often not possible over the
59 required temporal and spatial scale. Field studies have therefore to be complemented by hydro-
60 logical and soil erosion modeling studies. Hydrological and soil erosion models have been used
61 to predict the effect of land use and climate change on soil erosion and to identify hot spots of
62 soil erosion that require erosion control measures (Bossa et al., 2014; Hiepe, 2008; Pandey et
63 al., 2016). If available, LULC maps from different years may be used as input into hydrological
64 and soil erosion models to simulate the effect on runoff and soil erosion. Increased runoff and
65 soil erosion rates are often predicted by hydrological and soil erosion models if the natural vege-
66 tation is converted to arable land (Bossa, 2012; Hiepe, 2008; Yira et al., 2016).

67 Different model concepts exist (empirical, conceptual and physically based models) among
68 which physically based spatially distributed models are considered suitable for the analyses of
69 LULC impacts on erosion at smaller scales as a certain complexity is necessary for the predic-
70 tions of the changing LULC conditions (Pandey et al., 2016). The parameter values of these
71 model types have a physical meaning and therefore can be better estimated, which increases
72 the quality of the simulated output (de Vente et al., 2013; Merritt et al., 2003; Pandey et al.,
73 2016). The hydrological and soil erosion model SHETRAN (Birkinshaw et al., 2010b; Ewen et

74 al., 2000) has been successfully applied to simulate effects of changing LULC (Bathurst et al.,
75 2011; Lukey et al., 2000, 1995) and climate (Op de Hipt et al., 2018). SHETRAN studies used
76 several approaches to investigate the impacts of a changing LULC. On the one hand, hypothet-
77 ical scenarios derived from a simple change of vegetation properties (Bathurst et al., 2011,
78 2005; Birkinshaw et al., 2010a; Lukey et al., 2000, 1995) are used and on the other hand the
79 analyses of observed land use in different catchments were compared to reflect changed LULC
80 (Elliott et al., 2011). One novelty of the present study is therefore the combined investigation of
81 observed and future LULC change in the same catchment over more than 20 years using
82 SHETRAN.

83 The LULC change in the catchment is driven by a high population growth rate (3% per year)
84 leading to the expansion of cropland at the expense of savanna as it is frequently observed in
85 West Africa (CILSS, 2016; Codjoe, 2004; Yira et al., 2016). The principle motivation of the pre-
86 sent study is to fill the knowledge gap regarding the impact of LULC change on runoff generation
87 and soil erosion. Studies on these topics are rather limited in West Africa but work on the impact
88 of LULC change on hydrological processes (Yira et al., 2016) and on the general modeling of
89 soil erosion without changing LULC influences (Op de Hipt et al., 2017; Schmengler, 2010) in
90 the present study catchment exist. Despite these studies a clear knowledge gap was identified
91 regarding the assessment of past and future impacts of LULC change on soil erosion. Further-
92 more, the combined consideration of LULC and climate change is frequently identified as future
93 research objective (Op de Hipt et al., 2018; Yira, 2016). We aim to fill this gap by a combined
94 assessment of LULC and climate change over a period of 40 years (1990 – 2030). The
95 SHETRAN model was set up to simulate and to evaluate the impacts of these changes.
96 SHETRAN was already calibrated and validated in the present study catchment (Op de Hipt et
97 al., 2017).

98 The major aims of this study are, to:

- 99 1. Investigate the observed past and the modeled future LULC change using seven land
100 use maps.
- 101 2. Assess the isolated and combined impact of LULC and climate change on simulated
102 mean annual water yield and mean annual actual evapotranspiration.
- 103 3. Examine the isolated and combined effect of LULC and climate change on mean annual
104 suspended sediment yield and compare the contribution of different sediment sources
105 (land use, channel, hillslope).

106 **2 METHODS**

107 **2.1 Study area**

108 The studied catchment has a size of 126 km² and is located in the south-west of Burkina Faso,
109 West Africa (Figure 1). The study site is part of three focal watersheds of the WASCAL program
110 (West African Science Service Center on Climate Change and Adapted Land Use,
111 www.wascal.org). WASCAL is a multidisciplinary program investigating the influence of climate
112 and land use / land cover change on human and environmental systems.

113 The watershed is characterized by a slightly undulating landscape with low slope gradients (av-
114 erage and maximum gradients are 1.8° and 21°, respectively, Figure 1b) and an elevation
115 (Figure 1c) ranging from 269 to 504 m above sea level (masl). Annual precipitation range from
116 800 to 1200 mm/a for the period 1951 – 2005 (Schmengler, 2010). The annual rainfall dynamic
117 is characterized by a distinct rainy season (May to October) and a dry season from November to
118 April.

119 Soils are dominated by plinthosols (73%) according to the World Reference Base (WRB) for soil
120 resources (IUSS Working Group, 2006). Plinthosols are characterized by high content of coarse
121 particles and a plinthic subsurface layer. Soils of the valley bottoms are mainly gleysols. Other
122 soils formed in the region are cambisols, lixisols, leptosols and stagnosols (Figure 1e).

123 The natural vegetation is characterized by the Sudanian region with wood, shrub and
124 arboraceous savanna and abundant annual grasses. The growing population and the resulting
125 demand for cropland and settlements lead to a reduction of the savanna vegetation (Yira et al.,
126 2016). The dominant cultivated crops are sorghum (*Sorghum bicolor*), millet (*Pennisetum*
127 *glaucum*), maize (*Zea mays*), cowpeas (*Vigna unguiculata*) and groundnut (*Arachidis*
128 *hypogaea*). Cotton (*Gossypium hirsutum*) is the main cash crop.

129

130

131

132

133

134

135

136

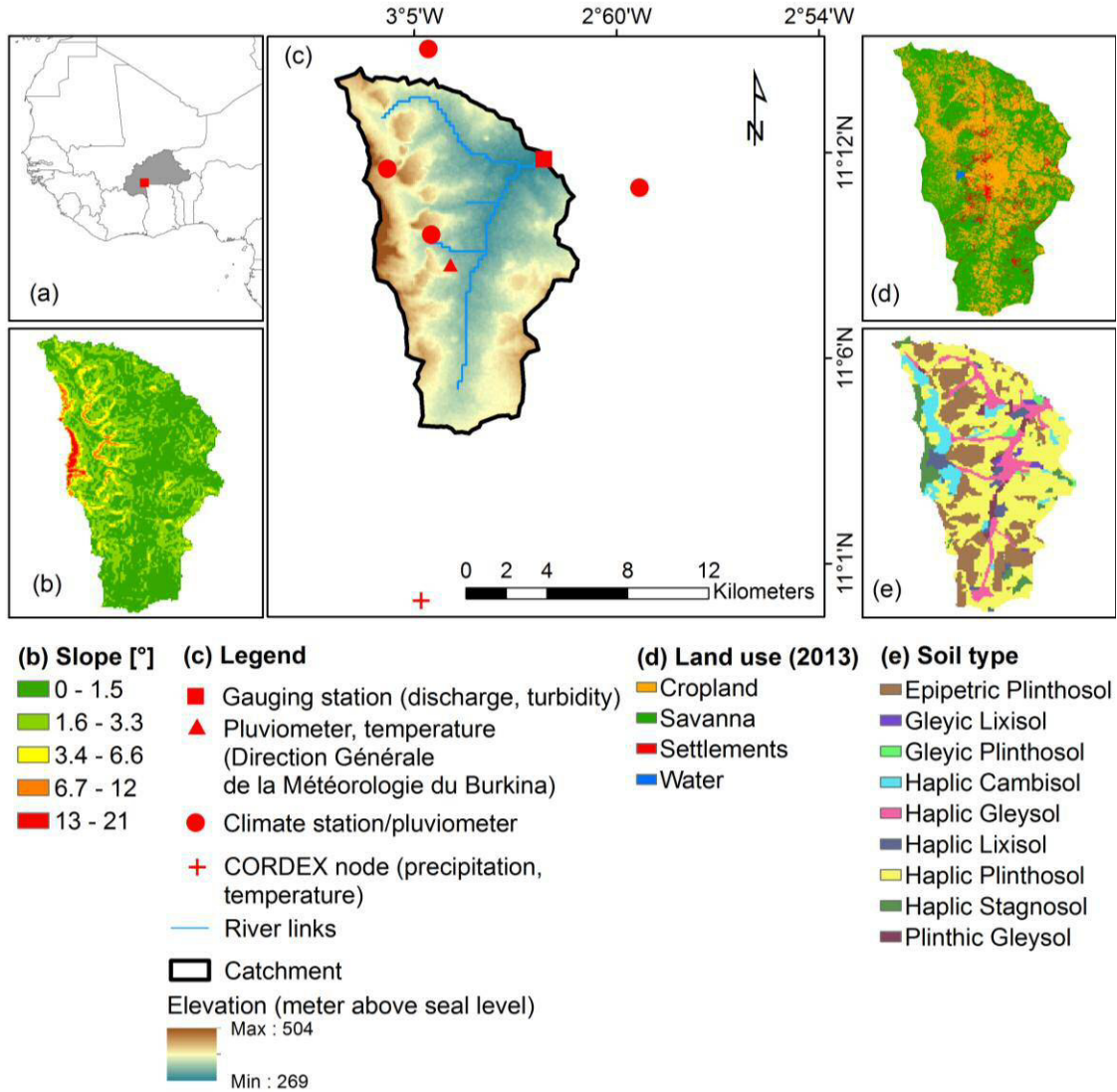


Figure 1: Location map of the Dano catchment: (a) location of the catchment and Burkina Faso in West Africa, (b) slope of the catchment, (c) model catchment, (d) land use map (Forkuor, 2014), (e) soil map (data base: soil survey done by Ozias Hounkpatin, Soil Science of Institute of Crop Science and Resource Conservation, University Bonn). DGM refers to the Direction Générale de la Météorologie du Burkina.

137 **2.2 Data sources and processing**

138 The modeling of changing surface runoff and soil erosion requires past, present and future cli-
139 mate and land use data as model inputs.

140 **2.2.1 Land use data**

141 Observed LULC maps

142 Observed LULC maps from four different years (LULC_1990, LULC_2000, LULC_2007,
143 LULC_2013) were available to assess the past impact of LULC change on hydrology and soil
144 erosion. The three maps that show the status from 1990 to 2007 were derived from Landsat TM
145 (<http://glovis.usgs.gov/>) and MODIS (<https://mrtweb.cr.usgs.gov/>) images by Landmann et al.
146 (2007). The map of 2013 compiled by Forkuor (2014) is based on Landsat TM and RapidEye
147 images (<https://www.planet.com/products/#satellite-imagery>). As the maps are available at dif-
148 ferent resolutions, they were resampled using the majority filter to match the resolution of 200 m.
149 Both studies used the Land Cover Classification System (LCCS) from the Food and Agricultural
150 Organization (FAO).

151 In order to homogenize the LULC classes for each of the four maps, the LULC classes of the
152 years 1990 to 2007 were reclassified to match the LULC map of the year 2013. The reclassifica-
153 tion was done based on the approach described in Yira et al. (2016): Classes with similar char-
154 acteristics regarding seasonality of vegetation cover and hydrological properties were grouped
155 (Table 1). The resulting land use maps were used to simulate the effect LULC change on water
156 and soil resources in the past.

157 Future LULC scenarios

158 Based on the observed LULC changes between 2000 and 2013, future LULC scenarios were
159 developed for the years 2019, 2025 and 2030 (LULC_2019, LULC_2025, LULC_2030) by using
160 the Land Change Modeler (Clark Labs, Clark University, Worcester, USA). The approach used

161 by the Land Change Modeler is based on transition potentials which are calculated using a Multi-
 162 Layer Perceptron (MLP) neural network (Chan et al., 2001). The transition potentials for the fu-
 163 ture depend on the transitions that have already occurred in the past. As explanatory variables
 164 several distance maps were used (distance to roads, fields and settlements) as well as spatially
 165 autocorrelated maps of the digital elevation model (DEM) and observed disturbances (transitions
 166 from savanna to crop or settlements). Finally a stochastic Markov chain technique (Wilson and
 167 Weng, 2011) is applied to simulate the probability of LULCC and generate the future land use
 168 maps.

169 As the prediction of the development of areas covered by surface water is difficult based on a
 170 very small proportion of grid cells, it was assumed that these areas have not changed since
 171 2013. An overview of the land use classes is given in Table 1.

Table 1: Initial LULC classes as given by Landmann et al. (2007) and Forkour (2014) and re-classified classes used in this study

Initial LULC classes	Proportional area [%] per year							Reclassified LULC classes
	1990	2000	2007	2013	2019	2025	2030	
Regularly flooded, woody, closed to open	1.03	29.2	-	-	-	-	-	Tree and shrub savannah
Broadleaved forest, closed, evergreen (>=65%)	1.77	-	-	-	-	-	-	Tree and shrub savannah
Woodland, closed (40 – 65%)	5.22	-	-	-	-	-	-	Tree and shrub savannah
Woodland closed/forest closed	59.3	-	8.80	-	-	-	-	Tree and shrub savannah
Reg. flooded, high confidence	1.16	-	-	-	-	-	-	Tree and shrub savannah
Burned area	4.03	2.64	-	-	-	-	-	Cropland
Bare soil scattered vegetation	1.00	-	-	-	-	-	-	Urban area
Regularly flooded wetland	0.84	-	-	-	-	-	-	Tree and shrub savannah
Herbaceous crops	8.28	-	-	-	-	-	-	Cropland
Herbaceous vegetation, closed (>=65%)	17.28	-	-	-	-	-	-	Tree and shrub savannah
Forest	-	3.45	15.5	-	-	-	-	Tree and shrub savannah
Grassland	-	35.1	46.7	-	-	-	-	Tree and shrub savannah
Cropland	-	16.1	20.4	36.3	42.3	48.3	54.5	Cropland
Wetland	-	13.2	1.52	-	-	-	-	Tree and shrub savannah
Urban area	-	0.16	6.54	5.19	7.19	9.19	11.1	Urban area
Water	-	-	0.42	0.39	0.39	0.39	0.39	Water

172 **2.2.2 Climate and hydrological data**

173 Two climate datasets were used in this study.

174 Observed climate and hydrological data

175 SHETRAN requires various input data to simulate hydrological and soil erosion processes
 176 (Table 2). Some of the required data sets are already available from previous studies and from
 177 literature. However, in order to calibrate and validate the model (see section 2.3.1) these data
 178 were complemented by a hydrological and meteorological measurement network that was in-
 179 stalled during the years 2012 to 2015. Five automatic weather stations including pluviometers
 180 were installed in the catchment. The outlet of the catchment was equipped with a water level and
 181 turbidity probe. Precipitation and calculated potential evapotranspiration (ETp) are given as
 182 hourly time series for each of the five climate stations located in the studied catchment.

183 Furthermore, an extensive soil survey was conducted to analyze physical and chemical soil
 184 properties and to retrieve the soil and hydrological parameters required by the model.

185 Observed climate data for the period 1990 – 2015 were used to assess the influence of LULC
 186 change on hydrology and soil erosion. To cover the full period we used data with a daily resolu-
 187 tion taken by the national meteorological service (Direction Général de la Météorologie du Burki-
 188 na, DGM) (Figure 1c).

189

190

Table 2: Applied datasets and required inputs for SHETRAN

Data set	Spatiotemporal resolution / scale	Source	Derived parameters
Topography	90 m	SRTM (Jarvis et al., 2008)	

Soil	1:25 000	Soil survey	Soil hydrological parameters (α , n^1 , K_{sat}^2 , θ_{sat}^3 , θ_{res}^4) texture etc.
Land use maps	5 to 250 m	Forkuor (2014), Landmann et al. (2007)	Land use type distribution
Land use characteristic		Literature	LAI ⁵ , Strickler coefficient, ETa/ETp ratio ⁶
Meteorological data	Hourly, Daily	Instrumentation WASCAL, DGM ⁷ , CORDEX ⁸	Rainfall, temperature, humidity, solar radiation, wind speed
Discharge	Hourly	Instrumentation WASCAL	Discharge
Erosion	Hourly, Event	Instrumentation WASCAL	Suspended sediment load, soil erosion rate

¹ α and n are van Genuchten empirical parameters, ² K_{sat} refers to the saturated hydraulic conductivity, ³ θ_{sat} to the saturated water content, ⁴ θ_{res} to the residual water content, ⁵LAI to the leaf area index and ⁶ETp/ETa ratio to the ratio of potential evapotranspiration to actual evapotranspiration, ⁷Direction Général de la Météorologie du Burkina, ⁸Coordinated Regional climate Downscaling Experiment project

191 Modeled climate data

192 Historical (1990 – 2005) and scenario-based (2006 – 2032) precipitation and temperature data
193 were retrieved from the regional climate model (RCM) CCLM4-8 (Climate Limited-area Modelling
194 Community, Germany) driven by the global climate model (GCM) ESM-LR (Max-Planck-Institute
195 for Meteorology, Germany). The Representative Concentration Pathways RCP 4.5 and RCP 8.5
196 (Moss et al., 2010) were used as future scenarios. The RCM-GCM simulation was run in the
197 framework of the Coordinated Regional climate Downscaling Experiment (CORDEX-Africa,
198 www.cordex.org). Due to the run time of SHETRAN the closest node and one climate model was
199 used only. The performance of other climate models and a discussion of the differences be-
200 tween nodes is given by Op de Hipt et al. (2018).

201 Historical precipitation and temperature data from CCLM-ESM model were compared with their
202 observed counterparts for the period 1971 – 2000 to control if the modeled variables are in
203 agreement with the observed. The modeled temperature shows a negative deviation compared
204 to the observed temperature (Figure 2a). As temperature is used to calculate potential evapo-
205 transpiration (Oudin et al., 2005) and has therefore strong effects on catchment hydrology, it was
206 bias corrected using the delta change approach described in Haddeland et al. (2012) (Figure
207 2b).

208 The comparison of modeled and observed precipitation indicates an obvious bias. Modeled pre-
209 cipitation is often higher than measured and a shift between the observed and the simulated
210 timing of the rainy season can be observed (Figure 2c). Therefore, a bias correction method was
211 used to correct the historical and future rainfall data derived from CCLM-ESM. The non-
212 parametric quantile mapping approach introduced by Gudmundsson et al. (2012) was applied.
213 The observed data were used to establish a transfer function which was applied to the historical
214 and the future rainfall data. The differences between mean monthly precipitation from all climate
215 models and the observed precipitation are considerably reduced after bias correction (Figure
216 2d).

217 The comparison of bias corrected precipitation and potential evapotranspiration between the
218 periods 1990 – 2005 and 2006 – 2032 shows an increase of precipitation by 5.4% to 7.8% and
219 an increase of ETp by 4.7% to 6%.

220 Because bias correction is done on monthly scale and because climate models simulate climate
221 and not weather, it cannot be expected that water and sediment fluxes using observed and
222 modelled climate are identical although the underlying climate variables precipitation and tem-
223 perature are statistically identical. Therefore, analysis of future climate can only be compared to
224 the modelled and not the observed past.

225

226

227

228

229

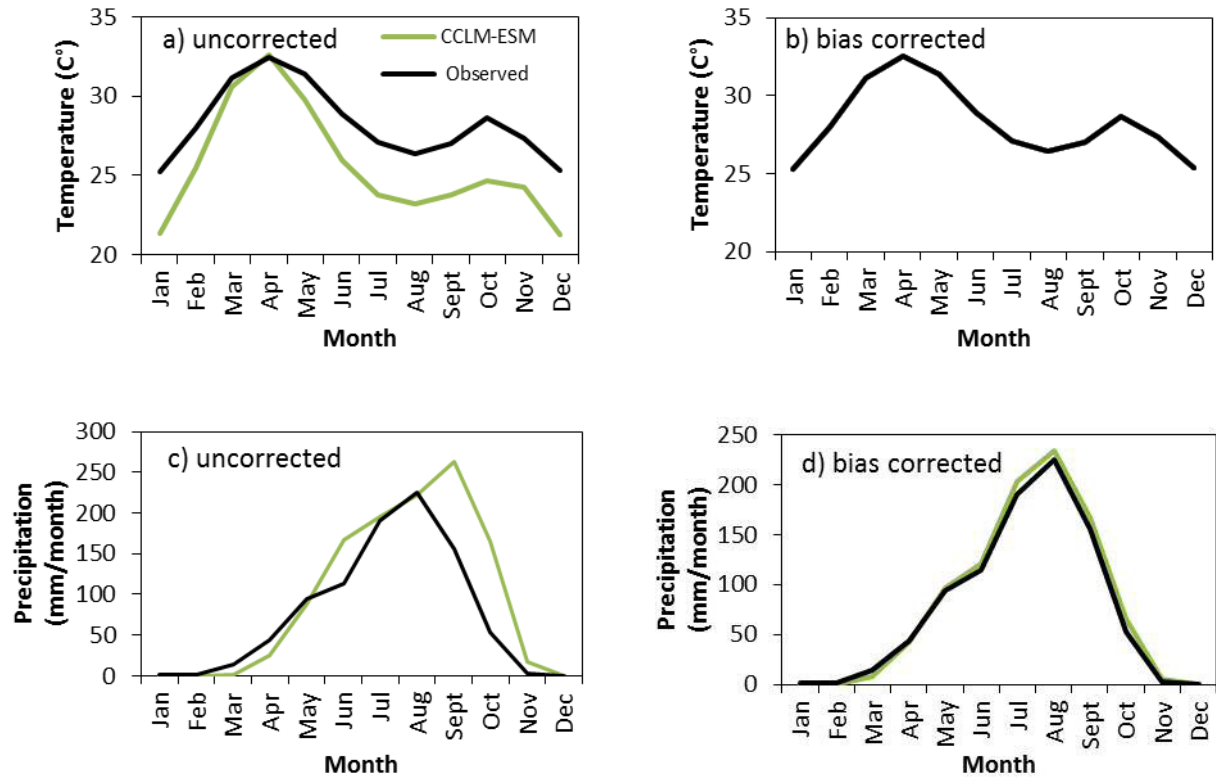


Figure 2: Uncorrected and bias corrected temperature (a, b) and precipitation (c, d).

230 2.3 Modeling approach

231 2.3.1 Model description, parameterization, calibration and validation

232 SHETRAN was selected in this study due to two main reasons. First, SHETRAN is able to simu-
 233 late erosion on hillslopes as well as in the river, which are both considered as important pro-
 234 cesses in the catchment. Second, it simulates processes based on continuous time series,
 235 which is necessary to use climate change scenarios and for land use comparisons over a given
 236 period. SHETRAN is a physically based spatially distributed hydrological soil erosion model. It is
 237 a derivative of SHE (Système Hydrologique Européen), which was jointly developed by the Brit-
 238 ish Institute of Hydrology, the Danish Hydraulic Institute and the French consulting company
 239 SOGREAH (Abbott et al., 1986). SHETRAN has been refined and complemented by new com-

240 ponents as e.g. the fully 3D simulation of subsurface water flow (Parkin, 1996) and sediment
241 transport (Wicks, 1988; Wicks and Bathurst, 1996). Detailed information is available online
242 (<http://research.ncl.ac.uk/shetran/>).

243 Details on model parameterization, calibration and validation are given in section 3.2 and Op de
244 Hipt et al. (2017). The parameterization of soil properties was done based on data obtained from
245 field measurements and additional literature analysis (Table 2, Table 3). Land use parameters
246 were taken from literature (see Table 3). Although SHETRAN comprises numerous parameters
247 that reflect the influence of the vegetation on hydrology we focused on two parameters: i) the
248 ratio of actual evapotranspiration (ET_a) to potential evapotranspiration (ET_p) and ii) the Strickler
249 coefficient (KSTR) that were reported to be sensitive regarding surface runoff (Bathurst et al.,
250 2004; Birkinshaw et al., 2010a; Đukić and Radić, 2016; Zhang, 2015). Erosion was described
251 using four parameters (overland flow and rain drop soil erodibility coefficients, channel bank
252 erodibility coefficient, threshold depth of loose sediment) that were adjusted based on literature
253 (Adams and Elliott, 2006; Birkinshaw et al., 2010a; de Figueiredo and Bathurst, 2007; Elliott et
254 al., 2011; Lukey et al., 2000, 1995; Norouzi Banis et al., 2004; Wicks and Bathurst, 1996) and
255 calibration (Table 3).

256 Spatially distributed data, including a digital elevation model (DEM), the soil and land use map
257 were used in a raster format with a grid resolution of 200 x 200 m. An extensive soil survey was
258 conducted to analyze physical and chemical soil properties and to retrieve the soil and hydrolog-
259 ical parameters required by the model.

260

261

262

263

Table 3: Soil, land use and erosion parameters in SHETRAN (NV: natural vegetation (mainly savannah), CR: crop land, SM: settlement)

Parameter	Description	Unit	Parameter range	Source
Hydrology				
ETa/ETp at field capacity (varies with land use type)	Ratio of actual evapotranspiration to potential evapotranspiration at field capacity	-	CR ¹ : 0.5 NV ² : 0.6 SM ³ : 0.1	Shuttleworth (1993)
KSTR (varies with land use type)	Strickler roughness coefficient	m ^{1/3} s ⁻¹	CR: 1.4 NV: 0.6 SM: 6.0	Mohamoud (1992), Shen and Julien (1993)
Soil erosion				
k_f (soil invariant)	Overland flow soil erodibility	kg m ⁻² s ⁻¹	7.5×10 ⁻¹¹	Calibration
k_r (varies with texture)	Raindrop soil erodibility coefficient	J ⁻¹	0.19 – 7.9	Adams and Elliott (2006), Birkinshaw et al. (2010a), de Figueiredo and Bathurst (2007), Elliott et al. (2011), Lukey et al. (2000, 1995), Norouzi Banis et al. (2004), Wicks and Bathurst (1996)
BKB (soil invariant)	Channel bank erodibility coefficient	kg m ⁻² s ⁻¹	1×10 ⁻⁶ – 3×10 ⁻⁶	Calibration
DLSMAX	Threshold depth of loose sediment	mm	1×10 ⁻⁶ – 9.9×10 ⁻⁶	Calibration

264

265 Although SHETRAN is physically based, land use and soil erosion related parameters needed to

266 be calibrated to adjust for model approximations and the spatial or temporal resolution of the

267 input data. In the present study six selected parameters (Table 3) were calibrated based on the

268 Latin Hypercube Sampling (LHS) methodology (McKay et al., 1979). Briefly, using LHS the pos-

269 sible multi-dimensional parameter space is sampled n times (usually n>100) in a stratified man-

270 ner and the parameters are used in the simulation model to determine behavioral simulations

271 (simulations which show an acceptable comparison with observed data). The hydrological com-

272 ponent of SHETRAN was calibrated based on the observed hydrograph from 2014 to 2015. The

273 soil erosion component was calibrated based on the observed suspended sediment load (SSL).

274 The model performance was statistically evaluated by the coefficient of determination (R²), the

275 Nash-Sutcliffe efficiency (NSE) (Nash and Sutcliffe, 1970) and the Kling-Gupta efficiency (KGE)

276 (Gupta et al., 2009; Kling et al., 2012) because a single quality measure is not sufficient for
277 model evaluation. The model was validated using data from the year 2015.

278 **2.3.2 Model application and simulations**

279 In this study, the model parameters and the boundary conditions remain unchanged for all simu-
280 lations. Therefore, LULC and climate change is not reflected by changing parameters but the
281 changing spatial patterns of the land cover classes and the changing climate data.

282 To evaluate the effects of changing land use and climate separately and their combined effects
283 we applied over all 17 model simulations. As the periods 1984 – 1996 and 1984 - 1989 were
284 used as the warm-up phase to reach hydrological equilibrium conditions, the period 1997 – 2032
285 (evaluation period) was used to evaluate the effect of LULC and climate change on average an-
286 nual water components and on the average annual specific sediment yield. For the model warm-
287 up climate data from 1984 to 1996 and the land use map LULC_1990 is applied. In order to
288 compare simulations we used different evaluation periods as shown in Table 4.

289 Statistical differences between the selected model outputs (water yield, actual evapotranspira-
290 tion, specific sediment yield) of each model run was investigated on a daily basis using the
291 Kruskal-Wallis test. Pairwise comparisons were studied by applying the Bonfferoni correction to
292 results of Mann-Whitney U tests.

293 The following points shortly describe each simulation. An overview of the different simulations is
294 given in Table 4.

295 The model simulations of the past (simulations M1_1990 – M5_90/13):

- 296 • The simulation M1_1990 is considered as the reference and applies the land use map
297 LULC_1990 over the entire simulation period (1990 – 2005). Observed climate data are used
298 to drive the simulation.

- 299 • Simulations M2_2000, M3_2007 and M4_2013 apply the observed land use maps from
300 2000, 2007 and 2013 to the period from 1997 to 2005. For each simulation the same ob-
301 served climate data for the period from 1997 to 2005 are used. During each simulation the
302 land cover did not change. Different simulation outputs are therefore the effect of different
303 LULC data only. To be able to compare simulations M1_1990 – M4_2013 with the simula-
304 tions driven by past modeled climate data, we limited the evaluation period to 1997 – 2005.
- 305 • The simulation M5_90/13 applies the chronological land use development as it has occurred
306 in the catchment. Therefore the LULC map from 1990 is applied to the period from 1990 to
307 1996, the map from 2000 applied to the period 1997 – 2003, the map from 2007 to the peri-
308 od 2004 – 2010 and finally the map from 2013 to the period 2011 – 2015. M5_90/13 uses
309 the same observed climate data as simulations M1 to M4.

310 The model simulations of the future (simulations M6_2019 – M17_90/13):

- 311 • Simulations M6_2019, M7_2025 and M8_2030 apply the modelled land use maps from
312 2019, 2025 and 2030 to the observed climate data from 1997 – 2005. In accordance with
313 simulations M2 to M4, during each simulation LULC does not change and changes between
314 each simulation are due to changing LULC, while each simulation applied the same ob-
315 served climate data.
- 316 • The simulations M9_1990_RCP4.5 and M10_1990_RCP8.5 use modeled climate data (see
317 section 2.2.2) of the period 1990 – 2032 in combination with the land use map LULC_1990
318 assuming a constant LULC since 1990. Model runs M9 and M10 use modeled climate data
319 and changes in fluxes are computed as differences between the modeled past (1990 – 2005)
320 and the modeled future (2006 – 2032). These simulations enable the assessment of climate
321 change as single factor. The periods 1990 – 2005 and 2006 – 2032 are compared regarding
322 the effect of climate change on discharge and SSY.

323 • A chronological and continuous application of all LULC maps (LULC_1990 – LULC_2030)
324 was only possible through the use of precipitation and temperature from a climate model
325 (see section 2.2.2). Modeled precipitation and temperature (1990 - 2032) in combination with
326 LULC maps from 1990 to 2030 were used to drive the simulations M11_90/30_RCP4.5 and
327 M12_90/30_RCP8.5. The periods 1990 – 2005 and 2006 – 2032 are compared regarding
328 the effect of climate change on discharge and SSY.

329 • Simulations M13_1990 – M17_90/13 are similar to simulations M1_1990 – M5_90/13 except
330 they use past modeled climate data from the period 1984 – 2005 and are necessary to eval-
331 uate the differences between the past modeled and observed climate data.

332

333

334

335

336

337

338

339

340

341

342

343

344

Table 4: LULC simulations, model periods and applied land use maps.

Data	Simulation name	Simulation period						
		Warm-up period	Evaluation period					
		1990 – 1996	1997 – 2005	-	-	-		
Observed climate and LULC maps	M1_1990	LULC_1990	LULC_1990	-	-	-		
	M2_2000	LULC_1990	LULC_2000	-	-	-		
	M3_2007	LULC_1990	LULC_2007	-	-	-		
	M4_2013	LULC_1990	LULC_2013	-	-	-		
		Warm-up period	Evaluation period					
		1990 – 1996	1997 – 2003	2004 – 2010	2011 – 2015			
	M5_90/13	LULC_1990	LULC_2000	LULC_2007	LULC_2013	-	-	-
Data	Simulation name	Warm-up period	Evaluation period					
		1990 – 1996	1997 – 2005					
Observed climate and modeled LULC maps	M6_2019	LULC_1990	LULC_2019	-	-	-		
	M7_2025	LULC_1990	LULC_2025	-	-	-		
	M8_2030	LULC_1990	LULC_2030	-	-	-		
Data	Simulation name	Warm-up period	Evaluation period					
		1990 - 1996	1997 – 2005	2006 – 2010	2011 – 2016	2017-2022	2023-2027	2028-2032
Modeled climate and observed LULC map	M9_1990_RCP4.5	LULC_1990	LULC_1990					
	M10_1990_RCP8.5	LULC_1990	LULC_1990					
Modeled climate and modeled LULC maps	M11_90/30_RCP4.5	LULC_1990	LULC_2000	LULC_2007	LULC_2013	LULC_2019	LULC_2025	LULC_2030
	M12_90/30_RCP8.5	LULC_1990	LULC_2000	LULC_2007	LULC_2013	LULC_2019	LULC_2025	LULC_2030
Data	Simulation name	Warm-up period	Evaluation period					
		1984 - 1997	1998 - 2005					
Past modeled climate and observed LULC maps	M13_1990	LULC_1990	LULC_1990					
	M14_2000	LULC_1990	LULC_2000					
	M15_2007	LULC_1990	LULC_2007					
	M16_2013	LULC_1990	LULC_2013					
		Simulation name	Warm-up period	Evaluation period				
			1984 - 1989	1990 - 1997	1998 - 2005			
	M17_90/13	LULC_1990	LULC_1990	LULC_2000				

345

346

347

348

349 Timestep sensitivity

350 The long term meteorological data operated by the national meteorological service (see Figure
351 1c) was only available on daily basis. This is critical since results of dynamic models such as
352 SHETRAN respond sensitively to the chosen simulation time step (Bruneau et al., 1995; Hessel,
353 2005; Yira, 2016; Zhang, 2015) and consequently the consideration of time and spatial scales is
354 fundamental in hydrological modeling (Blöschl and Sivapalan, 1995). Yira (2016) reports a de-
355 creasing modeled discharge with increasing time step. This can be explained by the information
356 loss during aggregation of rainfall data from sub-daily to daily resolution: It reduces the maxi-
357 mum intensities and therefore leads to an underestimation of overland flow due to infiltration
358 excess as this depends on rainfall intensity and soil infiltration rate. Consequently, simulated
359 discharge and hence sediment yield may be underestimated by the model. However, some
360 SHETRAN studies also use a daily timestep (de Figueiredo and Bathurst, 2007; Mourato et al.,
361 2015). Figure 3 shows that the exceedance probability does not change substantially between
362 two simulations with different timesteps. Although an increase in timestep reduces surface runoff
363 and sediment yield, this limitation cannot be avoided for the long-term simulations as no hourly
364 data are available. Because all scenarios are influenced by the same effect, conclusions drawn
365 from the analysis are not biased by the temporal resolution of the model runs.

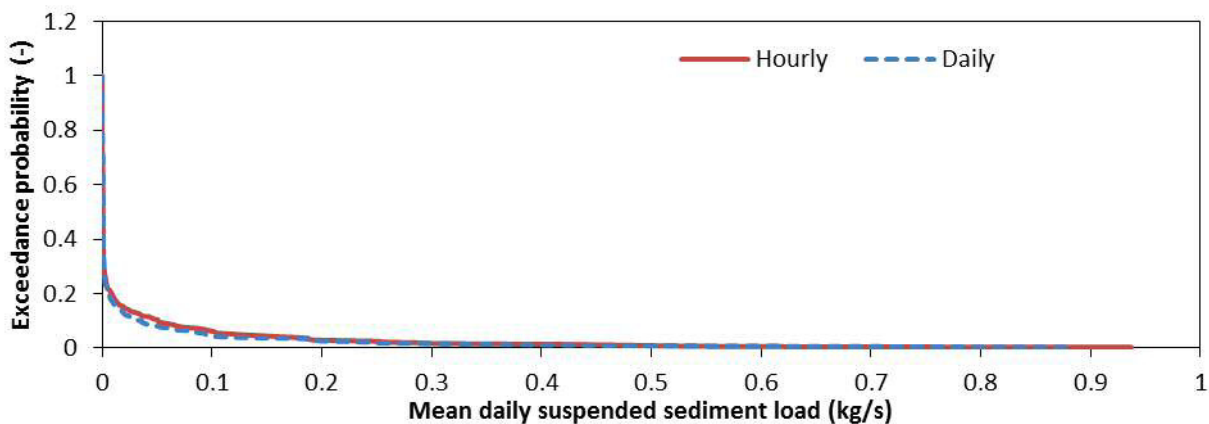


Figure 3: Exceedance probability of hourly and daily suspended sediment load

366 3 RESULTS AND DISCUSSION

367 3.1 Land use and land cover change

368 The LULC maps and changes of the period 1990 – 2030 are shown in Figure 4. The observed
369 LULC maps show an increase of mainly cropland and settlement area at the expense of savan-
370 na areas, which have decreased by almost 30% between 1990 (86.69%) and 2013 (58.12%)
371 whereas cropland has increased by almost 24% in the same period. An urbanization trend is
372 reflected by an increase in settlement areas by 4.1% between 1990 and 2013. The area covered
373 by surface water increases between 2000 and 2007 as the Moutouri reservoir was built in 2002.
374 The future LULC change (from 2019 to 2030) mainly follows the trend of the past. An increase of
375 cropland (42.2%) and settlement areas (10.19%) between 1990 and 2030 is opposed to a de-
376 crease in savanna by 52.7%.

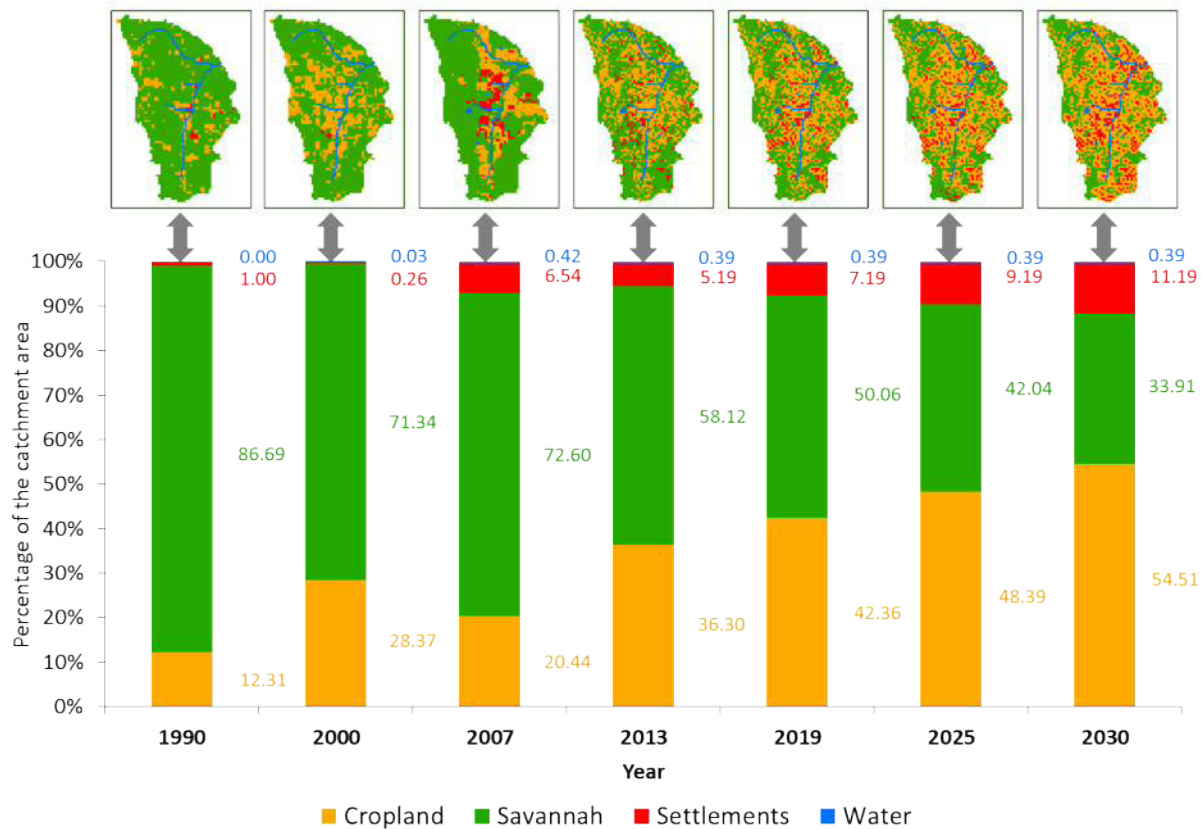


Figure 4: Observed (1990 – 2013) and modeled (2019 – 2030) LULC maps and the corresponding relative proportion of each land use.

377 Some inconsistencies are observed regarding the spatial distribution of settlements derived from
 378 the past LULC maps. Between 1990 and 2000 settlement areas in the LULC map are reduced
 379 due to the unlikely conversion of settlements to savanna, water and cropland. Further unlike
 380 LULC changes are noticed between the maps from 2000 and 2007 where the settlement area is
 381 25 fold increased over 7 years. The inconsistencies are of relatively low importance as the maximum
 382 proportion of cells characterized by an improbable change is < 7%. The LULC mapping of
 383 savanna areas is impeded due to the seasonality and the scattered LULC pattern (Cord et al.,
 384 2010; Forkuor, 2014). Therefore, the observed inconsistencies can be explained by a misclassification
 385 related to the difficulties of the LULC mapping of areas characterized by a distinct sea-

386 sonality (Wagner et al., 2013). Another reason may be the resampling of the maps needed to
387 attain the same grid resolution which discriminates the scattered land use classes (Yira et al.,
388 2016).

389 The large visual and numerical differences between LULC_2007 and the other maps rectified
390 the exclusion of LULC_2007 for the derivation of the future LULC maps. Two important issues
391 have to be discusses in this context: First, the future LULC development only depends on the
392 change that occurred between 2000 and 2013. Second, the future LULC may be afflicted with
393 large uncertainties because important variables as population growth and agronomical develop-
394 ments are not available to improve the predictions. However, based on observations from the
395 field and personal communication with local farmers, factors as the distance to the farm house
396 and the accessibility play an important role for cultivation.

397 An expansion of cropland at the expense of natural vegetation mainly due to increasing demand
398 for agricultural areas as a result of the population growth and national migration is also reported
399 by others (CILSS, 2016; Gray, 1999; Mahé et al., 2005; Ouedraogo et al., 2010; Paré et al.,
400 2008; Stephenne and Lambin, 2001; Thiombiano and Kampmann, 2010). The present study
401 assesses the increase of cropland by 0.95% per year while savanna is reduced by 1.14% per
402 year for the observed period (1990 – 2013). Paré et al. (2008) studied the influence of population
403 growth on land use change and reports conversion rates of 3.75% per year in the Sissili and Ziro
404 provinces, which are located in approximately 100 km distance to the study area. Although the
405 exact number differ the major driver controlling LULC change in the study area is population
406 growth and urbanization trends, which is also reported on the national level (CILLS, 2016). Fu-
407 ture LULC maps suggest an increase of cropland of 42.2% till 2030. This corresponds to the
408 scenarios used by Hiepe (2008) who reports increases between 56% – 119%. The deforestation
409 in the catchment is directly related to the growing demand in firewood used among others for the
410 production of local beer and remote areas are increasingly affected as the number of unprotect-
411 ed trees close to the main settlements diminishes. The logging of shea trees (*Vitellaria*

412 *paradoxa*) used to produce shea butter for export may pose a problem in the future as it is an
413 important financial income for small scale farmers. Another important cash crop is cotton whose
414 production has increased by 350% since 1990 (FAOSTAT, 2017).

415 **3.2 Performance of SHETRAN**

416 The performance of SHETRAN regarding the hydrological and erosion modeling is discussed in
417 Op de Hipt et al. (2017) and therefore only briefly summarized here. Based on the various per-
418 formance measures (sum of R^2 , KGE and NSE), several parameter sets gave satisfactory to
419 good quality measures according to the equifinality concept introduced by Beven and Freer
420 (2001). The given performance measures for discharge are in the range of 0.7 and 0.79 for cali-
421 bration and between 0.66 and 0.76 for validation which is comparable to other studies that used
422 SHETRAN (e.g. Birkinshaw et al., 2014; Đukić and Radić, 2016, 2014; Mourato et al., 2015;
423 Naseela et al., 2015; Tripkovic, 2014; Zhang, 2015). Among these studies R^2 and NSE values
424 above 0.5 are frequently reported. Larger differences between simulated and observed dis-
425 charge occur during low flow conditions where the observed discharge is frequently underesti-
426 mated by the model. This is not surprising since low flow was not in the focus and consequently
427 parameters controlling low flow such as K_{sat} in sub-surface soils were not considered during the
428 calibration. Overestimated peaks during the rainy season can be attributed to the spatial as-
429 signment of climate stations, which was done using Thiessen polygons. This method may not be
430 appropriate to account for localized precipitation events. Nevertheless, alternative interpolations
431 methods like inverse distance weighting and Kriging may also be inadequate to reflect local
432 storms as they smooth rainfall intensities over larger spatial extends.

433 In terms of erosion rates the NSE is 0.4 and 0.2 and the R^2 is 0.47 and 0.37 for calibration and
434 validation of SSL respectively. These results are in the range of other studies (de Figueiredo and
435 Bathurst, 2007; Elliott et al., 2011; Zhang, 2015) and comparable with other erosion models (de

436 Vente et al., 2013; Jetten et al., 1999). Given the various sources of measurement uncertainty a
437 NSE of larger than 0.7 can't be expected (de Vente et al., 2013).

438 **3.3 Land use and climate change effects**

439 **3.3.1 Hydrology**

440 Figure 5a, Table 5, and Table 6 show the influence of land use on simulated mean annual water
441 yield over the considered period (1997 – 2030). The simulations that were driven by the past
442 observed climate and LULC maps (M1_1990 – M5_90/13) indicate an increased water yield by
443 3.6% (M2_2000) to 46.4% (M3_2007) (evaluation period: 1997 – 2005). The water yield of the
444 continuous simulation M5_90/13 is 20.3% higher compared to M1_1990 (evaluation period 1997
445 – 2015). It shows that LULC change over almost 20 years has affected the water balance of the
446 studied catchment significantly.

447 Simulations driven by future modeled LULC maps and observed climate data (M6_2019 –
448 M8_2030) show highest increases in discharge between 52.4% – 91.6% compared to M1_1990
449 (evaluation period: 1997 – 2005). Consequently, the predicted LULC change will lead to an in-
450 creased discharge assuming a similar climate development as observed between 1990 and
451 2005.

452 Simulations M9_1990_RCP4.5 and M10_1990_RCP8.5 are driven by modeled climate data and
453 the map LULC_1990 only, assuming no change of LULC since 1990. The comparison between
454 simulated discharge of the period 1990 – 2005 and of the period 2006 – 2032 shows an increase
455 of discharge between 24.5% (M10_1990_RCP8.5) and 46.7% (M9_1990_RCP4.5). The in-
456 creased water yield is attributed to climate change only.

457 Simulations M11_90/30_RCP4.5 and M12_90/30_RCP8.5 are driven by a combined LULC and
458 climate change. The comparisons of the periods 1990 – 2005 to the years 2006 - 2032 show
459 high increases (50.5% (M12) – 73.4% (M11)) of discharge. Consequently, the combined devel-

460 opment of climate and LULC may intensify the future change of hydrological conditions in the
461 catchment.

462 Simulations M13 – M17 use past observed LULC maps and past modeled climate data. Accord-
463 ingly, these simulations are needed to assess the influence of past modeled climate data and
464 LULC change on water and sediment yield. M14_2000 – M16_2013 show increases between
465 3.4% (M14) and 16.6% (M16) compared to M13_1990 (evaluation period: 1997 – 2005). The
466 continuous simulation M17_90/13 show an increase of 1.5% compared to M13_1990 (evaluation
467 period: 1990 – 2005)

468 The comparison between the groups M9/M10 (climate change only, +24.5% – +46.7%),
469 M11/M12 (LULC and climate change, +50.5 – +73.4%) and M13-M17 (LULC change only,
470 +1.5% – +16.6%) shows that LULC change only leads to increases in water yield. When com-
471 paring LULC change and climate change alone it is clear that climate change has a larger im-
472 pact but LULC amplifies climate change impacts strongly. However, future LULC (2019 – 2030)
473 will have a stronger impact as currently observed. Furthermore, the comparison between M13 -
474 M17 and M1-M5 shows that the simulation driven by observed climate data (M1 – M5) are char-
475 acterized by higher percental increases than those simulations that are driven by modeled cli-
476 mate data from the past although precipitation is higher for M13-M17. The differences in relative
477 change between the group M1-M5 and M13-M17 is related to differences in the absolute dis-
478 charge which is about three times higher for M13-M17. Therefore, M13-M17 show a smaller
479 relative change compared to M1-M5.

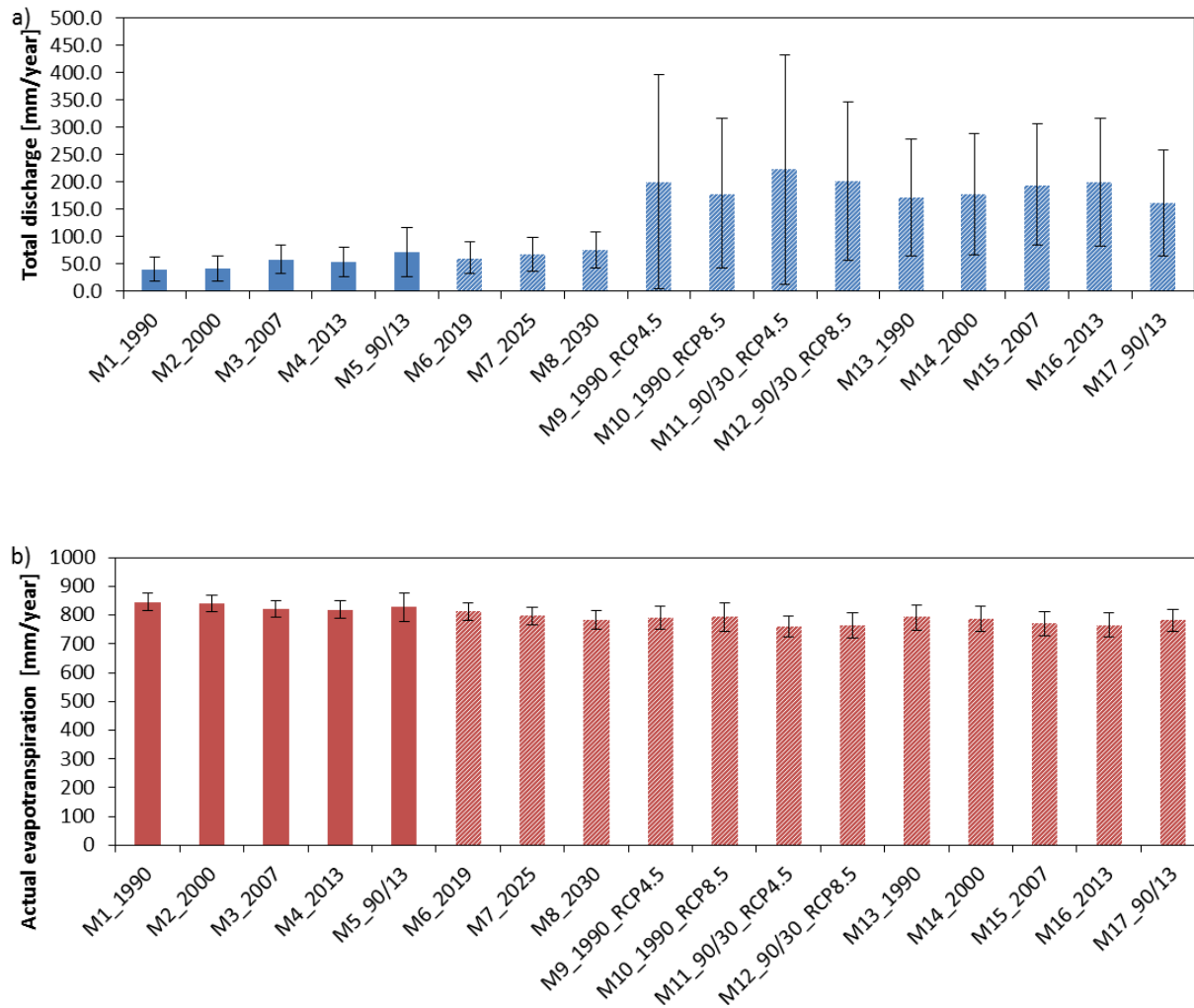


Figure 5: a) Mean annual total water yield for M1_1990 – M12_90/30_RCP8.5 and b) mean annual actual evapotranspiration for simulations M1_1990 – M12_90/30_RCP8.5. Error bars indicate the standard deviation calculated based on annual sums. Dashed bars indicate the use of modeled LULC and/or climate. See Tab. 4 and the text for explanation of the different scenarios

480 Statistically significant ($p < 0.0007$) differences exist between almost all pairs. Exceptions are
 481 M1_1990/M5_2013, M3_2007/M4_2013, and M11_90/30_RCP4.5/M12_90/30_RCP8.5.

482 The effect of LULC and climate change on ETa is shown in Figure 5b. The simulations driven by
 483 observed data (M1_1990 – M5_90/13) indicate that ETa decreases between 0.7% and 3.2%.

484 Simulations that used modeled LULC maps and observed climate data (M6_2019 – M8_2030)
485 show decreasing ETa (4% – 7.3%) compared to M1_1990 (evaluation period: 1997 – 2005). The
486 simulations that use climatic predictions assuming constant LULC since 1990 (M9, M10) show
487 an increasing ETa by between 3.1% (M9) and 3.3% (M10). A decreasing trend is predicted by
488 the combined consideration of LULC and climate change as shown by simulations M11 (-1.58%)
489 and M12 (-0.96%). Simulations M14_2000 – M17_90/13 show the same trend as simulations
490 M2-M5 with decreasing rates of ETa between 0.3% and 3.4%. The comparison between the
491 pairs M9/M10 and M11/M12 suggests that LULC change may dominate the impact on ETa be-
492 cause the increasing trend as suggested by climate change only is reversed by the combined
493 consideration of LULC and climate change. Significant ($p < 0.0007$) differences compared to the
494 reference the simulation M1_1990 exist for the majority of considered pairs.

495 The presented figures for simulations M1_1990 – M5_90/13 are similar to the results of Yira et
496 al. (2016) who studied the influence of a changing LULC on the hydrology in the same area
497 based on similar data using WASiM (Water Balance Simulation Model). He observed an in-
498 crease in discharge of 20% between M1_1990 and M5_90/13. The general trend of increasing
499 discharge and decreasing ETa is reported by others and LULC change was frequently responsi-
500 ble for this development (Bossa et al., 2014; Cornelissen et al., 2013; Mahé et al., 2005; Roudier
501 et al., 2014; Yira et al., 2016). Bossa et al. (2014) studied the impact of climate and LULC
502 change on hydrology in the Ouémé catchment in Benin. They assess the effect of different LULC
503 scenarios on water yield to be between +3% and +8%. For the combined consideration of cli-
504 mate and LULC change they report a decreasing water yield over the period 2015 – 2019 ac-
505 cording to the negative future precipitation signal. The influence of the future precipitation signal
506 on water yield is also confirmed by Yira et al. (2017) and by the present study as CCLM-ESM
507 shows a positive future signal for the considered period (2006 – 2032). However, conclusions
508 drawn from simulations that use data from climate models have to be considered carefully as
509 uncertainties of future precipitation predictions are large (Yira et al., 2017). Simulations M9 and

510 M10 are afflicted with large inter-annual variabilities as indicated by the high standard deviation.
511 These variabilities are a result from the precipitation as predicted by CCLM-ESM.

512 Regarding the consideration of LULC change only, the presented results are confirmed by ex-
513 periments conducted on smaller scales. These experiments suggest that the increase of water
514 yield due to land use change is attributed to a change of soil properties such as a decreasing
515 K_{sat} leading to Hortonian surface runoff (Giertz et al., 2005; Yira, 2016). However, in SHETRAN
516 K_{sat} varies with soil type and not with land use. Consequently, it remained unchanged over all
517 simulations and cannot explain the differences between the simulations. Among the land use
518 specific model parameters LAI, the vegetation cover fraction, the Strickler roughness coefficient
519 (KSTR), and the ratio ET_a/ET_p were adjusted to the corresponding land use types to reflect their
520 differences regarding the hydrological effects. In SHETRAN the roughness coefficient and the
521 ratio ET_a/ET_p have distinct effects on discharge as shown by Op de Hipt et al. (2017) and Đukić
522 and Radić (2016). Decreased surface roughness as observed on agricultural fields (Engman,
523 1986) results in higher surface runoff velocities and therefore especially influences the runoff
524 peaks. However, interactions between surface roughness, infiltration and evapotranspiration
525 also lead to a change of water yield. The ratio ET_a/ET_p , which depends on the vegetation type
526 and varies with soil water tension, has strong effects on the water balance components. A higher
527 actual evapotranspiration on natural land use types is frequently reported (e.g. Compaoré,
528 2006). Other vegetation properties such as LAI or vegetation cover also influence the discharge.
529 Decreasing LAI and vegetation cover leads to more throughfall, which may increase surface
530 runoff.

Table 5: Average annual water balance and specific suspended sediment yield of simulation driven by observed climate. The evaluation period from 1997 – 2005 is marked by *, the evaluation period from 1997 – 2015 is marked by **

Simulation	M1_1990	M2_2000	M3_2007	M4_2013	M5_90/13	M6_2019	M7_2025	M8_2030
Mean annual rainfall [mm]	877*/903**	877*/903**	877*/903**	877*/903**	903**	877*/903**	877*/903**	877*/903**
Mean annual ETp [mm]	1826*/1809*	1826*/1809*	1826*/1809*	1826*/1809*	1809**	1826*/1809*	1826*/1809*	1826*/1809*
Mean annual ETa [mm]	846*/844**	840*/839**	821*/820**	818*/820**	827**	812*/822**	797*/802**	784*/786**
Mean annual water yield [mm]	39.4*/59.4**	40.8*/61.7**	57.7*/81.2**	52.7*	71.4**	60*/86.7**	67.1*/95.5**	75.5*/105**
Mean annual specific suspended sediment yield [t/ha]	0.021*/0.0317**	0.021*/0.0312**	0.032*/0.0449**	0.031*/0.0445**	0.0395**	0.038*/0.0531**	0.043*/0.0599**	0.051*/0.0684**

531

532

533

534

535

536

537

538

539

Table 6: Average annual water balance and specific suspended sediment yield. Annual means of the modeled past (1990 – 2005)^{a)} and the modeled scenarios (2006 – 2032)^{b)} are indicated for simulations M9 – M12. The evaluation period from 1998 – 2005 for M13-M17 is marked by *, the evaluation period from 1998 – 2015 is marked by **

Simulation	M9_1990_RCP4.5	M10_1990_RCP8.5	M11_90/30_RCP4.5	M12_90/30_RCP8.5	M13_1990	M14_2000	M15_2007	M16_2013	M17_90/2005
Mean annual rainfall [mm]	951 ^{a)} – 1026 ^{b)}	951 ^{a)} – 1002 ^{b)}	951 ^{a)} – 1026 ^{b)}	951 ^{a)} – 1002 ^{b)}	997*/951**	997*/951**	997*/951**	997*/951**	951**

Mean annual ETP [mm]	1578 ^{a)} – 1653 ^{b)}	1578 ^{a)} – 1674 ^{b)}	1578 ^{a)} – 1653 ^{b)}	1578 ^{a)} – 1674 ^{b)}	1616*/157 8**	1616*/157 8**	1616*/157 8**	1616*/157 8**	1578**
Mean annual ETa [mm]	775 ^{a)} – 799 ^{b)}	775 ^{a)} – 801 ^{b)}	768 ^{a)} – 756 ^{b)}	768 ^{a)} – 761 ^{b)}	798*/784**	794*/780**	776*/763**	771*/758**	781**
Mean annual water yield [mm]	154 ^{a)} – 226 ^{b)}	154 ^{a)} – 192 ^{b)}	152 ^{a)} – 264 ^{b)}	152 ^{a)} – 229 ^{b)}	170.6*/157 .9**	176.5*/164 .7**	194.3*/182 .3**	198.9*/187 .5**	160.4**
Mean annual specific suspended sediment yield [t/ha]	0.084 ^{a)} – 0.13 ^{b)}	0.084 ^{a)} – 0.11 ^{b)}	0.082 ^{a)} – 0.15 ^{b)}	0.082 ^{a)} – 0.13 ^{b)}	0.097*/0.0 9**	0.099*/0.1 02**	0.112*/0.1 1**	0.120*/0.0 87**	0.087**

540

541 3.3.2 Soil erosion

542 Figure 6, Table 5 and Table 6 show the effect of LULC and climate change on the mean annual
543 specific suspended sediment yield (SSY). Simulations driven by observed data (M1_1990 –
544 M5_90/13) show a change of SSY between -3.3% (M2_2000) and +52.6% (M3_2007) for the
545 evaluation period 1997 - 2005. The relative contribution of each land use type to the catchment
546 erosion varies between M1_1990 to M5_90/13 (evaluation period: 1997 – 2015): The relative
547 contribution of cropland increases by 11% whereas the contribution of savanna decreases by
548 9% as a result of the changing proportion of each land use type. The channel contribution varies
549 between 42% (M4_2013) and 51% (M1_1990) suggesting that if the contribution of hillslope ero-
550 sion increases the channel contribution decreases. Among the sediment sources water also con-
551 tributes to the sediment yield of the catchment. The model structure only allows a limited number
552 of soil types and an additional soil type reflecting the conditions of areas covered by water could
553 not be implemented. The continuous simulation M5_90/13 exhibits an increase of 24.7% com-
554 pared to the reference simulation M1_1990 suggesting that LULC change has already a pro-
555 nounced impact on soil erosion (evaluation period: 1997 – 2015).

556 Simulations driven by future modeled LULC maps and observed climate data (M6_2019 –
557 M8_2030) show highest increases in SSY between 78.5% (M6_2019) and 138.4% (M8_2030)
558 compared to M1_1990 (evaluation period: 1997 – 2005). Consequently, the predicted LULC
559 change will lead to an increased SSY assuming a similar climate development as observed be-
560 tween 1990 and 2005. The proportion of the different sources remains roughly similar between
561 M6 – M8 except for savanna whose contribution decreases by 6%.

562 The simulation M9_1990_RCP4.5 and M10_1990_RCP8.5 reflect a changing climate assuming
563 stable LULC since 1990. The periods 1990 – 2005 and 2006 – 2032 are used for the compari-
564 son. The simulations show that the predicted change in precipitation (+5.4% to +7.8%), ETa
565 (+3.1% to +3.3%) and accordingly water yield (+24.5% to +46.7%) strongly influence SSY. Both,
566 water yield and SSY are strongly correlated as surface runoff is the principal driver of sediment
567 transport. Overall SSY is predicted to increase by 31.1% (M10_1990_RCP8.5) and 54.7%
568 (M9_1990_RCP4.5). Table 5 shows that these increases are especially attributed to the scenar-
569 io-based predictions (2005 – 2030). Furthermore, the source distribution indicates that these
570 increases are especially caused by a substantial increase of channel contribution compared to
571 the other simulations.

572 The continuous simulations M11_90/30_RCP4.5 and M12_90/30_RCP8.5 reflect the combined
573 impact of LULC and climate change on SSY. Overall SSY is predicted to increase by 67.7%
574 (M12_90/30_RCP8.5) to 90.1% (M11_90/30_RCP4.5) compared to the period 1990 – 2005.

575 Simulations M14_2000 – M16_2013 show increases by between 2.1% and 23.3% compared to
576 simulation M13_1990 (evaluation period: 1997 – 2005). These changes are lower compared to
577 the results of simulations M1-M5 although absolute precipitation is higher for M13-M17. This is
578 attributed to the absolute amount of SSY which almost 3 times higher for simulation M13-
579 M15. Simulation M17_90/13 are driven by past modeled climate data and observed LULC maps
580 of 1990 and 2000. The relative change between M13 and M17 is almost 0%.

581 The comparison between the groups M9/M10 (climate change only, +31.1 – +54.7%), M11/M12
582 (climate and LULC change, +67.7% – +90.1%) and M13 - M17 (LULC change only, 0% -
583 +23.3%) suggest that LULC change may have a large impact on SSY. Simulations driven by
584 climate change only (M9/M10) show higher increases than those simulations that were driven by
585 LULC change (M13 – M17). However, climate change impacts are significantly amplified by
586 LULC change as shown by simulations M11/M12.. All of the discussed simulations are statisti-

587 cally different except the pairs M3/M4 and M11/M12. However, uncertainties of LULC and cli-
 588 mate predictions have to be discussed. Simulations M9 to M12 are characterized by high inter-
 589 annual variabilities. This is mostly related to large uncertainties of predicted precipitation. The
 590 impact of climate change on the rainfall pattern and temperature in West Africa is difficult to as-
 591 sess and differences between climate models regarding amplitude and direction exists (Kasei et
 592 al., 2010; Niang et al., 2014). This uncertainty is among others attributed to the difficulties of
 593 simulating convective rainfalls and the rainfalls generated by the West African Monsoon (WAM)
 594 which is attributed to the incomplete knowledge of the WAM, lack of observations and the natu-
 595 ral climate variability in the region (Cook, 2008; Druyan et al., 2010; Field and Barros, 2014;
 596 Klein et al., 2015; Niang et al., 2014).

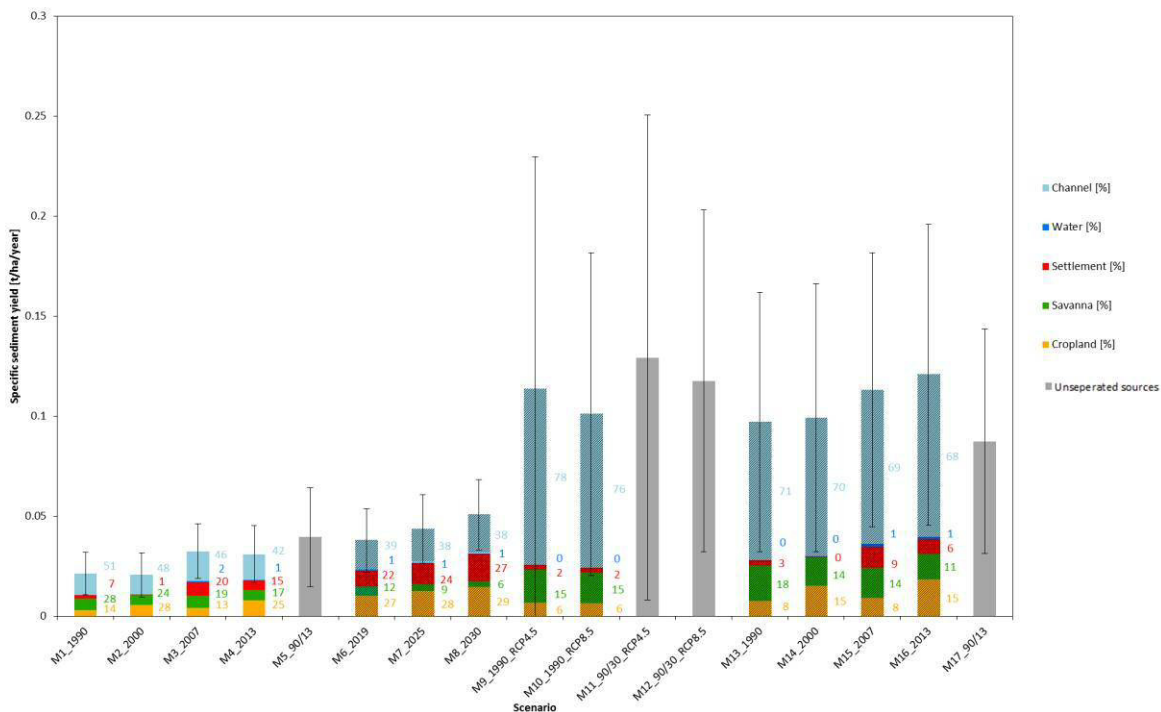


Figure 6: Mean annual specific suspended sediment yield for the simulations M1_1990 – M12_90/30_RCP8.5. The contribution of each source is given in % for all simulations except for the continuous simulations (M5, M11, M12, M17). Error bars indicate the standard deviation cal-

culated based on annual sums. Dashed bars indicate the use of modeled LULC maps and/or modeled climate data.

597 From Figure 6 and the described results it can be concluded that LULC and climate change are
598 important drivers that control the catchment sediment yield and the corresponding erosion
599 sources. Increased erosion rates following a conversion from natural vegetation to cropland are
600 frequently confirmed by measurements and simulations in the region (e.g. Bossa et al., 2014;
601 Giertz et al., 2005; Hiepe, 2008). Giertz et al. (2005) compared the influence of different crops
602 and natural vegetation on soil erosion and concluded that increased surface runoff on cropland
603 resulted in increased soil loss on agricultural fields compared to the savanna environment. The
604 increased surface runoff can be explained by the reduction of macroporosity as result of de-
605 creased biological activity following the disturbance of the soil by agricultural activities. Further-
606 more, farming leads to a decreased soil quality parameters (Braimoh and Vlek, 2004) as e.g. a
607 loss of soil organic matter which destabilizes soil aggregates and facilitates surface crusting re-
608 sulting in a decreased infiltration rate (Descroix et al., 2009; Valentin et al., 2004). However, this
609 process chain is not simulated by SHETRAN. Bossa et al. (2014) investigated the effect of LULC
610 and climate change on sediment yield in the Ouémé catchment in Benin. Their modeling ap-
611 proach included the SWAT model, climate data from REMO and five LULC maps from 2003 to
612 2029. The combined application of LULC and climate change suggests an increase of SSY by
613 6% to 41% (Bossa et al., 2014). Differences between their results and ours can be explained by
614 the different climate model (CCLM-ESM vs. REMO) and by the different modeling approach
615 (SHETRAN vs. SWAT).

616 The simulated specific sediment yields are quite low for all simulations (< 0.13 t/ha). In this con-
617 text it is important to notice, that we consider the suspended fraction only. Furthermore, the term
618 soil erosion is differentiated from sediment yield. Soil erosion refers to soil detachment and not
619 necessarily soil loss from a specific area. Sediment yield refers to the amount of eroded soil that

620 is transported to a certain point in the catchment. However, the simulated suspended sediment
621 yields are comparable with specific suspended sediment yields measured in 2014 (0.04 – 0.13
622 t/ha/year) especially if the large simulated inter-annual variability is considered. The problem of
623 low simulated SSY is already discussed in Op de Hipt (2017) and may also be attributed to the
624 parameterization of the erosion component and the insufficient representation of space and time
625 in the model approach. However, the adjustment of the erosion parameters in a way that they
626 reflect the natural conditions is quite challenging due to limited knowledge of the parameter
627 ranges and of the erosion processes and source distribution especially in West Africa.
628 Schmengler (Schmengler, 2010; Schmengler and Vlek, 2015) studied soil erosion in the same
629 catchment by comparing sedimentation rates in 3 headwater sub-catchments (7.9 – 23.6 km²).
630 Two of her studied headwater catchments show lower SSY (0.3 t/ha/year – 0.8 t/ha/year). They
631 are representative of the typical flat terrain (2° – 3°). The third headwater catchment is located in
632 the western part and is characterized by steeper slope gradients (up to 20°) which leads to sub-
633 stantially higher SSY (4.4 t/ha/year). The mean slope of our study catchment is 1.8 and therefore
634 comparable to the two catchments showing a low annual SSY. The differences compared to our
635 results can be explained by the different fractions considered and the topographical position.
636 Schmengler (2015) investigated reservoirs located in the headwater areas. Consequently, her
637 measured SSY is only valid for these topographical positions and possible sedimentation
638 downslope is not considered.

639 The contribution of channels to the mean annual SSY seems to be quite high (51 – 76%) for all
640 simulations. However, recent results from fingerprinting analyses which were conducted in 2013
641 and 2014 support the modeling result for the past. The contribution of subsurface sources rang-
642 es 44% and 47% (Michael Rode, personal communication, 14th July 2017).

643 4 CONCLUSION

644 The present study investigated the LULC and climate change in the Dano catchment and its
645 effects on catchment hydrology and soil erosion using the process based SHETRAN model,
646 which was driven by past (observed) and future (modeled) LULC maps and modeled and ob-
647 served climate data. The main results of this study are:

648 1. The most important land use change in the catchment is the conversion from savanna to
649 cropland. The study of the observed LULC maps (1990 – 2013) shows an annual con-
650 version rate of savanna of 1.14% since 1990. The future LULC maps (2019 – 2030) pre-
651 dict an increase of cropland by 42.2% compared to 1990.

652 2. The analysis of the isolated impact of the LULC change on catchment hydrology clearly
653 suggests an increase of mean annual water yield (3.6% – 91.6%) and a decrease of
654 mean annual ETa (0.7 – 7.3%) while the proportion of cropland increases. The compari-
655 son between simulations suggests that the impact of future climate (24.5 – 46.7%) may
656 be amplified by the inclusion of LULC change (50.5 – 73.4%). However, uncertainties of
657 climate model outputs have to be considered. The combined effect of LULC and climate
658 change leads to a decrease in ETa (0.96% – 1.58%).

659 3. The investigation of the isolated effect of LULC changes on specific suspended sediment
660 yield (SSY) over the period 1990 – 2030 mostly shows an increasing trend (-3.6 -
661 138.4%) which is supported by measurements and modeling studies. The increase of
662 SSY is mostly attributed to the enlarging cropland, which also forms an important and
663 growing contribution source to total catchment erosion. The comparison of the isolated
664 impact of climate change and the combined effect of climate and LULC change suggest
665 that the inclusion of LULC change may amplified the climate change impacts. The com-
666 bined impact of LULC and climate change results in high changes of SSY (+67.7% –
667 +90.1%).

668 The obtained modeling results highlight the negative effects of the conversion of natural vegeta-
669 tion to cropland or settlements on catchment hydrology and soil loss independent whether ob-
670 served or modeled past climate data were used. The conversion results in less infiltration, higher
671 surface runoff and soil loss as well as lower groundwater recharge. However, the present find-
672 ings are based on results of hydrological and soil erosion modeling driven by LULC and climate
673 data which are subject to uncertainties. The observed LULC maps were produced based on dif-
674 ferent satellite products and needed to be reclassified. The afflicted uncertainties are propagated
675 as these maps are the basis for the development of future LULC scenarios. The precipitation as
676 modeled by climate models is frequently considered as uncertain as shown by comparison stud-
677 ies. Furthermore, the modeling approach is based on the changing spatial proportion of the dif-
678 ferent land use types only and does not consider the complex processes and feedback loops
679 between land use changes, soil properties, hydrology, and soil erosion. Consequently, the re-
680 sults must be carefully interpreted even if the model was validated in terms of discharge and
681 suspended sediment load. A focus should be put to relative and not the absolute comparisons
682 between the simulations. This relative comparison signals a clear effect of LULC and climate
683 change on hydrology and soil erosion.

684 In addition to the related uncertainties possible implications need to be discussed. The predicted
685 changes of the hydrological cycle and the altered sediment budget may have implications for
686 different fields as for example agricultural productivity or water availability. However, a discus-
687 sion based on measured data is beyond the scope and possibilities of the present work. There-
688 fore, the following discussion of possible implications includes results from previous studies.

689 A clear link has been identified between soil erosion, soil fertility, agricultural production and food
690 security (Niang et al., 2014; Pimentel, 2006). Garcia-Fayos and Bochet (2009) studied the im-
691 pact of climate change on the interaction between soil erosion and different soil and vegetation
692 properties in semiarid Mediterranean shrublands in eastern Spain. Their analyses suggest that
693 the negative impact of climate change and increased soil erosion on vegetation properties (spe-

694 cies richness and plant cover) negatively affects soil erodibility, nutrient content and water hold-
695 ing capacity which may lead to a decline of soil and agricultural productivity. The negative impact
696 of climate change on soil erosion and agricultural yields was proven by Zhang et al. (2004) for
697 experimental sites in Oklahoma, USA. They used modelled climate data and the WEPP model to
698 simulate the effect of climate change on soil erosion and wheat yield. A similar study was con-
699 ducted by Li et al. (2011) for the Loess Plateau in China. Their results suggest that plant yields
700 may increase despite increased erosion rates due to the fertilization effects of CO₂. Paeth et al.
701 (2008) studied the impact of climate change on soil degradation and agricultural production in
702 Benin using REMO data and predict a decline in crop yield of up to 23% due to soil erosion. A
703 similar range of projected decreasing yields are reported by Butt et al. (2005) for Mali. Our re-
704 sults show that it is not possible to identify a clear positive or negative trend regarding the future
705 erosion rates. Therefore, it is also difficult to consult decision makers regarding adaption strate-
706 gies for an appropriate agricultural management. Based on the studies presented above we can
707 conclude that a climate or LULC induced increase of erosion rates may have negative effects on
708 soil fertility, agricultural production and ultimately food security. Thus, governmental support of
709 soil and water conservation measures such as stone lines, intercropping or the traditional Zai
710 system (Roose et al., 1999) would be necessary to increase the environmental resilience of this
711 region. In view of the low SSY on hillslopes and the large contribution of channel erosion as
712 simulated by SHETRAN (Figure 6) it may be questionable if the increased erosion rates will sig-
713 nificantly affect agricultural production. Our modeling results and findings from a recent finger-
714 printing campaign suggest that a substantial part (about 50%) of the sediment loss in the catch-
715 ment results from bank erosion and river incision. However, the above mentioned conservation
716 techniques may also decrease surface runoff and hence discharge in the channels which in turn
717 may lead to decreased bank erosion and river incision. This would also decrease the off-site
718 effects on reservoirs located downstream as reservoir siltation is recognized as a serious prob-
719 lem (Schmengler, 2010).

720 However, it is debatable if results from modeling studies conducted on a rather large scale and
721 coarse temporal and spatial resolution can be used to derive specific advices for decision mak-
722 ers on the local scale because these results are rather valid on the catchment scale and do not
723 perfectly reflect the local diversity regarding the catchment properties but also the different pro-
724 cesses. As such SHETRAN considers already important processes but some observations from
725 the field are not well reflected. This considers for example the role of inland valleys which are
726 rather sediment sinks for material eroded on upstream as observations from the field suggest.
727 Furthermore, these observations suggest that soil properties and erosion processes differ on
728 very small scales and the coarse spatial resolution we had to use may limit the transfer from
729 model results to locally implementable advices for decision makers. Therefore, the current mod-
730 elling study underlines future research demands for climate model projections with smaller un-
731 certainties. As specific advices for decision makers should be based on several independent
732 research studies we also emphasize the need for further research regarding feedback loops
733 between climate change, LULC change, soil erosion and.

734

735 **5 ACKNOWLEDGEMENTS**

736 The authors are grateful for the financial support provided by the German Federal Ministry of
737 Education and Research (BMBF) (Grant No.01LG1202E) under the auspices of the West African
738 Science Service Centre for Climate Change and Adapted Land Use (WASCAL) project. Fur-
739 thermore, we thank Stephen Birkinshaw (School of Engineering, Newcastle University) for his
740 kind support regarding the set-up of SHETRAN. We acknowledge the soil sampling and map-
741 ping done by Ozias Hounkpatin (Soil Science of Institute of Crop Science and Resource Con-
742 servation, University Bonn). We also thank the CORDEX project and partner institutions for mak-
743 ing climate data available and D. Wisser for providing a R-code for bias correction.

744 **6 REFERENCES**

- 745 Abbott, M.B., Bathurst, J.C., Cunge, J.A., O'Connell, P.E., Rasmussen, J., 1986. An introduction
746 to the European Hydrological System — Systeme Hydrologique Europeen, "SHE", 1: His-
747 tory and philosophy of a physically-based, distributed modelling system. *Journal of Hy-*
748 *drology* 87, 45–59. [https://doi.org/10.1016/0022-1694\(86\)90114-9](https://doi.org/10.1016/0022-1694(86)90114-9)
- 749 Adams, R., Elliott, S., 2006. Physically based modelling of sediment generation and transport
750 under a large rainfall simulator. *Hydrological Processes* 20, 2253–2270.
751 <https://doi.org/10.1002/hyp.6050>
- 752 Bathurst, J.C., Birkinshaw, S.J., Cisneros, F., Fallas, J., Iroumé, A., Iturraspe, R., Novillo, M.G.,
753 Urciuolo, A., Alvarado, A., Coello, C., Huber, A., Miranda, M., Ramirez, M., Sarandón, R.,
754 2011. Forest impact on floods due to extreme rainfall and snowmelt in four Latin Ameri-
755 can environments 2: Model analysis. *Journal of Hydrology* 400, 292–304.
756 <https://doi.org/10.1016/j.jhydrol.2010.09.001>
- 757 Bathurst, J.C., Ewen, J., Parkin, G., O'Connell, P.E., Cooper, J.D., 2004. Validation of catchment
758 models for predicting land-use and climate change impacts. 3. Blind validation for internal
759 and outlet responses. *Journal of Hydrology* 287, 74–94.
760 <https://doi.org/10.1016/j.jhydrol.2003.09.021>
- 761 Bathurst, J.C., Moretti, G., El-Hames, A., Moaven-Hashemi, A., Burton, A., 2005. Scenario mod-
762 elling of basin-scale, shallow landslide sediment yield, Valsassina, Italian Southern Alps.
763 *Nat. Hazards Earth Syst. Sci.* 5, 189–202. <https://doi.org/10.5194/nhess-5-189-2005>
- 764 Beven, K., Freer, J., 2001. Equifinality, data assimilation, and uncertainty estimation in mecha-
765 nistic modelling of complex environmental systems using the GLUE methodology. *Jour-*
766 *nal of Hydrology* 249, 11–29. [https://doi.org/10.1016/S0022-1694\(01\)00421-8](https://doi.org/10.1016/S0022-1694(01)00421-8)
- 767 Birkinshaw, S.J., Bathurst, J.C., Iroumé, A., Palacios, H., 2010a. The effect of forest cover on
768 peak flow and sediment discharge — an integrated field and modelling study in central-
769 southern Chile. *Hydrological processes* 25, 1284–1297. <https://doi.org/10.1002/hyp.7900>
- 770 Birkinshaw, S.J., Bathurst, J.C., Robinson, M., 2014. 45 years of non-stationary hydrology over a
771 forest plantation growth cycle, Coalburn catchment, Northern England. *Journal of Hy-*
772 *drology* 519, Part A, 559–573. <https://doi.org/10.1016/j.jhydrol.2014.07.050>
- 773 Birkinshaw, S.J., James, P., Ewen, J., 2010b. Graphical user interface for rapid set-up of
774 SHETRAN physically-based river catchment model. *Environmental Modelling & Software*
775 25, 609–610. <https://doi.org/10.1016/j.envsoft.2009.11.011>
- 776 Blöschl, G., Sivapalan, M., 1995. Scale issues in hydrological modelling: A review. *Hydrological*
777 *Processes* 9, 251–290. <https://doi.org/10.1002/hyp.3360090305>
- 778 Bossa, A., 2012. Multi-scale modeling of sediment and nutrient flow dynamics in the Ouémé
779 catchment (Benin) - towards an assessment of global change effects on soil degradation
780 and water quality (Phd thesis). Rheinische Friedrich-Wilhelms-Universität Bonn, Bonn
781 <<http://hss.ulb.uni-bonn.de/2012/2983/2983.htm>>.
- 782 Bossa, A., Diekkrüger, B., Agbossou, E., 2014. Scenario-Based Impacts of Land Use and Cli-
783 mate Change on Land and Water Degradation from the Meso to Regional Scale. *Water*
784 6, 3152–3181. <https://doi.org/10.3390/w6103152>
- 785 Braimoh, A.K., Vlek, P.L.G., 2004. The impact of land-cover change on soil properties in north-
786 ern Ghana. *Land Degradation & Development* 15, 65–74. <https://doi.org/10.1002/ldr.590>
- 787 Bruneau, P., Gascuel-Oudou, C., Robin, P., Merot, P., Beven, K., 1995. Sensitivity to space and
788 time resolution of a hydrological model using digital elevation data. *Hydrological Pro-*
789 *cesses* 9, 69–81. <https://doi.org/10.1002/hyp.3360090107>
- 790 Butt, T.A., McCarl, B.A., Angerer, J., Dyke, P.T., Stuth, J.W., 2005. The economic and food se-
791 curity implications of climate change in Mali. *Climatic Change* 68, 355–378.
792 <https://doi.org/10.1007/s10584-005-6014-0>

- 793 Chan, J.C., Chan, K., Yeh, A.G., 2001. Detecting the Nature of Change in an Urban Environ-
794 ment: A Comparison of Machine Learning Algorithms. *Photogrammetric Engineering &*
795 *Remote Sensing* 67, 213–225.
- 796 CILSS (Comité Inter-états de Lutte contre la Sécheresse dans le Sahel), 2016. Landscapes of
797 West Africa - A Window on a Changing World. U.S. Geological Survey EROS, Garretson,
798 United States.
- 799 Codjoe, S.N.A., 2004. Population and Land Use, Cover Dynamics in the Volta River Basin of
800 Ghana: 1960-2010. Cuvillier Verlag.
- 801 Compaoré, H., 2006. The impact of savannah vegetation on the spatial and temporal variation of
802 the actual evapotranspiration in the Volta Basin, Navrongo, Upper East Ghana. Cuvillier.
- 803 Cook, K.H., 2008. Climate science: The mysteries of Sahel droughts. *Nature Geoscience* 1,
804 647–648. <https://doi.org/10.1038/ngeo320>
- 805 Cord, A., Conrad, C., Schmidt, M., Dech, S., 2010. Standardized FAO-LCCS land cover map-
806 ping in heterogeneous tree savannas of West Africa. *Journal of Arid Environments* 74,
807 1083–1091. <https://doi.org/10.1016/j.jaridenv.2010.03.012>
- 808 Cornelissen, T., Diekkrüger, B., Giertz, S., 2013. A comparison of hydrological models for as-
809 sessing the impact of land use and climate change on discharge in a tropical catchment.
810 *Journal of Hydrology* 498, 221–236. <https://doi.org/10.1016/j.jhydrol.2013.06.016>
- 811 de Figueiredo, E.E., Bathurst, J.C., 2007. Runoff and sediment yield predictions in a semiarid
812 region of Brazil using SHETRAN, in: Proceedings of the PUB Kick-off Meeting. Present-
813 ed at the PUB Kick-off meeting, IAHS, Brasilia, Brazil.
- 814 de Vente, J., Poesen, J., Verstraeten, G., Govers, G., Vanmaercke, M., Van Rompaey, A.,
815 Arabkhedri, M., Boix-Fayos, C., 2013. Predicting soil erosion and sediment yield at re-
816 gional scales: Where do we stand? *Earth-Science Reviews* 127, 16–29.
817 <https://doi.org/10.1016/j.earscirev.2013.08.014>
- 818 Descroix, L., Mahé, G., Lebel, T., Favreau, G., Galle, S., Gautier, E., Olivry, J.C., Albergel, J.,
819 Amogu, O., Cappelaere, B., 2009. Spatio-temporal variability of hydrological regimes
820 around the boundaries between Sahelian and Sudanian areas of West Africa: A synthe-
821 sis. *Journal of Hydrology* 375, 90–102. [10.1016/j.jhydrol.2008.12.012](https://doi.org/10.1016/j.jhydrol.2008.12.012).
- 822 Diekkrüger, B., 2010. Hydrological processes and soil degradation in Benin, in: Speth, P.,
823 Christoph, M., Diekkrüger, B. (Eds.), *Impacts of Global Change on the Hydrological Cy-
824 cle in West and Northwest Africa*. Springer, Berlin.
- 825 Druyan, L.M., Feng, J., Cook, K.H., Xue, Y., Fulakeza, M., Hagos, S.M., Konaré, A., Moufouma-
826 Okia, W., Rowell, D.P., Vizy, E.K., Ibrah, S.S., 2010. The WAMME regional model
827 intercomparison study. *Climate Dynamics* 35, 175–192. [https://doi.org/10.1007/s00382-
828 009-0676-7](https://doi.org/10.1007/s00382-009-0676-7)
- 829 Đukić, V., Radić, Z., 2016. Sensitivity Analysis of a Physically Based Distributed Model. *Water
830 Resources Management* 30, 1669–1684. <https://doi.org/10.1007/s11269-016-1243-8>
- 831 Đukić, V., Radić, Z., 2014. GIS Based Estimation of Sediment Discharge and Areas of Soil Ero-
832 sion and Deposition for the Torrential Lukovska River Catchment in Serbia. *Water Re-
833 sources Management* 28, 4567–4581. <https://doi.org/10.1007/s11269-014-0751-7>
- 834 Elliott, A.H., Oehler, F., Schmidt, J., Ekanayake, J.C., 2011. Sediment modelling with fine tem-
835 poral and spatial resolution for a hilly catchment. *Hydrological Processes* 26, 3645–3660.
836 <https://doi.org/10.1002/hyp.8445>
- 837 Engman, E.T., 1986. Roughness coefficients for routing surface runoff. *Journal of Irrigation and
838 Drainage Engineering* 112, 39–53. [https://doi.org/10.1061/\(ASCE\)0733-
839 9437\(1986\)112:1\(39\)](https://doi.org/10.1061/(ASCE)0733-9437(1986)112:1(39))
- 840 Ewen, J., Parkin, G., O'Connell, P.E., 2000. SHETRAN: distributed river basin flow and transport
841 modeling system. *Journal of Hydrologic Engineering* 5, 250–258.
842 [https://doi.org/10.1061/\(ASCE\)1084-0699\(2000\)5:3\(250\)](https://doi.org/10.1061/(ASCE)1084-0699(2000)5:3(250))
- 843 FAOSTAT, 2017. Burkina Faso [WWW Document]. URL
844 <http://www.fao.org/faostat/en/#country/233> (accessed 2.16.17).

845 Field, C.B., Barros, V.R. (Eds.), 2014. Climate change 2014: impacts, adaptation, and vulnerabil-
846 ity. Cambridge University Press, New York, NY.

847 Forkuor, G., 2014. Agricultural Land Use Mapping in West Africa Using Multi-sensor Satellite
848 Imagery (Phd thesis). Julius-Maximilians-Universität, Würzburg, Germany
849 <<https://opus.bibliothek.uni-wuerzburg.de/frontdoor/index/index/docId/10868>>.

850 García-Fayos, P., Bochet, E., 2009. Indication of antagonistic interaction between climate
851 change and erosion on plant species richness and soil properties in semiarid Mediterra-
852 nean ecosystems. *Global Change Biology* 15, 306–318. <https://doi.org/10.1111/j.1365-2486.2008.01738.x>

854 Giertz, S., Hiepe, C., Steup, G., Sintondji, L., Diekkrüger, B., 2010. Hydrological processes and
855 soil degradation in Benin, in: Speth, P., Christoph, M., Diekkrüger, B. (Eds.), *Impacts of
856 Global Change on the Hydrological Cycle in West and Northwest Africa*. Springer, Berlin.

857 Giertz, S., Junge, B., Diekkrüger, B., 2005. Assessing the effects of land use change on soil
858 physical properties and hydrological processes in the sub-humid tropical environment of
859 West Africa. *Physics and Chemistry of the Earth, Parts A/B/C* 30, 485–496.
860 <https://doi.org/10.1016/j.pce.2005.07.003>

861 Gray, L.C., 1999. Is land being degraded? A multi scale investigation of landscape change in
862 southwestern Burkina Faso. *Land Degradation & Development* 10, 329–343.
863 [https://doi.org/10.1002/\(SICI\)1099-145X\(199907/08\)10:4<329::AID-LDR361>3.0.CO;2-I](https://doi.org/10.1002/(SICI)1099-145X(199907/08)10:4<329::AID-LDR361>3.0.CO;2-I)

864 Gudmundsson, L., Bremnes, J.B., Haugen, J.E., Engen-Skaugen, T., 2012. Technical Note:
865 Downscaling RCM precipitation to the station scale using statistical transformations - a
866 comparison of methods. *Hydrology and Earth System Sciences* 16, 3383–3390.
867 <https://doi.org/10.5194/hess-16-3383-2012>

868 Gupta, H.V., Kling, H., Yilmaz, K.K., Martinez, G.F., 2009. Decomposition of the mean squared
869 error and NSE performance criteria: Implications for improving hydrological modelling.
870 *Journal of Hydrology* 377, 80–91. <https://doi.org/10.1016/j.jhydrol.2009.08.003>

871 Haddeland, I., Heinke, J., Voß, F., Eisner, S., Chen, C., Hagemann, S., Ludwig, F., 2012. Effects
872 of climate model radiation, humidity and wind estimates on hydrological simulations. *Hy-
873 drology and Earth System Sciences* 16, 305–318. <https://doi.org/10.5194/hess-16-305-2012>

875 Hessel, R., 2005. Effects of grid cell size and time step length on simulation results of the Lim-
876 burg soil erosion model (LISEM). *Hydrological Processes* 19, 3037–3049.
877 <https://doi.org/10.1002/hyp.5815>

878 Hiepe, C., 2008. Soil degradation by water erosion in a sub-humid West-African catchment - a
879 modelling approach considering land use and climate change in Benin (Phd thesis).
880 Rheinische Friedrich-Wilhelms-Universität Bonn, Bonn, <[http://hss.ulb.uni-
881 bonn.de/2008/1628/1628.htm](http://hss.ulb.uni-bonn.de/2008/1628/1628.htm)>.

882 IUSS Working Group, 2006. World reference base for soil resources 2006, 2nd ed, World Soil
883 Resources Reports. FAO, Rome, Italy.

884 Jarvis, A., Reuter, H.I., Nelson, A., Guevara, E., 2008. Hole-filled SRTM for the globe Version 4.
885 available from the CGIAR-CSI SRTM 90m Database (<http://srtm.csi.cgiar.org>).

886 Jetten, V., de Roo, A., Favis-Mortlock, D., 1999. Evaluation of field-scale and catchment-scale
887 soil erosion models. *CATENA* 37, 521–541. [https://doi.org/10.1016/S0341-8162\(99\)00037-5](https://doi.org/10.1016/S0341-8162(99)00037-5)

889 Kasei, R., Diekkrüger, B., Leemhuis, C., 2010. Drought frequency in the Volta Basin of West
890 Africa. *Sustainability Science* 5, 89–97. <https://doi.org/10.1007/s11625-009-0101-5>

891 Klein, C., Heinzeller, D., Bliefenicht, J., Kunstmann, H., 2015. Variability of West African mon-
892 soon patterns generated by a WRF multi-physics ensemble. *Climate Dynamics* 45,
893 2733–2755. <https://doi.org/10.1007/s00382-015-2505-5>

894 Kling, H., Fuchs, M., Paulin, M., 2012. Runoff conditions in the upper Danube basin under an
895 ensemble of climate change scenarios. *Journal of Hydrology* 424–425, 264–277.
896 <https://doi.org/10.1016/j.jhydrol.2012.01.011>

- 897 Landmann, T., Herty, C., Dech, S., Schmidt, M., Dech, S., Schmidt, M., Vlek, P., 2007. Land
898 cover change analysis within the GLOWA Volta basin in West Africa using 30-meter
899 Landsat data snapshots, in: 2007 IEEE International Geoscience and Remote Sensing
900 Symposium. Presented at the International Geoscience and Remote Sensing Symposi-
901 um, Barcelona, pp. 5298–5301. <https://doi.org/10.1109/IGARSS.2007.4424058>
- 902 Li, Z., Liu, W.-Z., Zhang, X.-C., Zheng, F.-L., 2011. Assessing the site-specific impacts of climate
903 change on hydrology, soil erosion and crop yields in the Loess Plateau of China. *Climatic*
904 *Change* 105, 223–242. <https://doi.org/10.1007/s10584-010-9875-9>
- 905 Lukey, B., Sheffield, J., Bathurst, J., Hiley, R., Mathys, N., 2000. Test of the SHETRAN tech-
906 nology for modelling the impact of reforestation on badlands runoff and sediment yield at
907 Draix, France. *Journal of Hydrology* 235, 44–62. [https://doi.org/10.1016/S0022-1694\(00\)00260-2](https://doi.org/10.1016/S0022-1694(00)00260-2)
- 909 Lukey, B.T., Sheffield, J., Bathurst, J.C., Lavabre, J., Mathys, N., Martin, C., 1995. Simulating
910 the effect of vegetation cover on the sediment yield of mediterranean catchments using
911 SHETRAN. *Physics and Chemistry of the Earth* 20, 427–432.
912 [https://doi.org/10.1016/0079-1946\(95\)00056-9](https://doi.org/10.1016/0079-1946(95)00056-9)
- 913 Mahé, G., Paturel, J.-E., Servat, E., Conway, D., Dezetter, A., 2005. The impact of land use
914 change on soil water holding capacity and river flow modelling in the Nakambe River,
915 Burkina-Faso. *Journal of Hydrology* 300, 33–43.
916 <https://doi.org/10.1016/j.jhydrol.2004.04.028>
- 917 McKay, M.D., Beckman, R.J., Conover, W.J., 1979. A Comparison of Three Methods for Select-
918 ing Values of Input Variables in the Analysis of Output from a Computer Code.
919 *Technometrics* 21, 239–245. <https://doi.org/10.2307/1268522>
- 920 Merritt, W.S., Letcher, R.A., Jakeman, A.J., 2003. A review of erosion and sediment transport
921 models. *Environ. Modell. Softw.* 18, 761–799. [https://doi.org/10.1016/S1364-8152\(03\)00078-1](https://doi.org/10.1016/S1364-8152(03)00078-1)
- 923 Mohamoud, Y.M., 1992. Evaluating Manning's roughness coefficients for tilled soils. *Journal of*
924 *Hydrology* 135, 143–156. [https://doi.org/10.1016/0022-1694\(92\)90086-B](https://doi.org/10.1016/0022-1694(92)90086-B)
- 925 Moss, R.H., Edmonds, J.A., Hibbard, K.A., Manning, M.R., Rose, S.K., van Vuuren, D.P., Carter,
926 T.R., Emori, S., Kainuma, M., Kram, T., Meehl, G.A., Mitchell, J.F.B., Nakicenovic, N.,
927 Riahi, K., Smith, S.J., Stouffer, R.J., Thomson, A.M., Weyant, J.P., Wilbanks, T.J., 2010.
928 The next generation of scenarios for climate change research and assessment. *Nature*
929 463, 747–756. <https://doi.org/10.1038/nature08823>
- 930 Mourato, S., Moreira, M., Corte-Real, J., 2015. Water Resources Impact Assessment Under
931 Climate Change Scenarios in Mediterranean Watersheds. *Water Resources Manage-*
932 *ment* 29, 2377–2391. <https://doi.org/10.1007/s11269-015-0947-5>
- 933 Naseela, E.K., Dodamani, B.M., Chandran, C., 2015. Estimation of Runoff Using NRCS-CN
934 Method and SHETRAN Model. *International Advanced Research Journal in Science, En-*
935 *gineering and Technology* 2, 23–28. <https://doi.org/10.17148/IARJSET.2015.2807>
- 936 Nash, J.E., Sutcliffe, J.V., 1970. River flow forecasting through conceptual models part I — A
937 discussion of principles. *Journal of Hydrology* 10, 282–290. [https://doi.org/10.1016/0022-1694\(70\)90255-6](https://doi.org/10.1016/0022-1694(70)90255-6)
- 939 Niang, I., Ruppel, O.C., Abdrabo, M.A., Essel, A., Lennard, C., Padgham, J., Urquhart, P., 2014.
940 Africa, in: Barros, V.R., Field, C.B., Dokken, D.J., Mastrandrea, M.D., Mach, K.J., Bilir,
941 T.E., Chatterjee, M., Ebi, K.L., Estrada, Y.O., Genova, R.C., Girma, B., Kissel, E.S.,
942 Levy, A.N., MacCracken, S., Mastrandrea, P.R., White, L.L. (Eds.), *Climate Change*
943 *2014: Impacts, Adaptation, and Vulnerability. Part B: Regional Aspects.* Cambridge Uni-
944 *versity Press, Cambridge, United Kingdom and New York, NY, USA, pp. 1199–1265.*
- 945 Norouzi Banis, Y., Bathurst, J.C., Walling, D.E., 2004. Use of caesium-137 data to evaluate
946 SHETRAN simulated long-term erosion patterns in arable lands. *Hydrological Processes*
947 18, 1795–1809. <https://doi.org/10.1002/hyp.1447>

- 948 Op de Hipt, F., Diekkrüger, B., Steup, G., Yira, Y., Hoffmann, T., Rode, M., 2018. Modeling the
949 impact of climate change on water resources and soil erosion in a tropical catchment in
950 Burkina Faso, West Africa. *CATENA* 163, 63–77.
951 <https://doi.org/10.1016/j.catena.2017.11.023>
- 952 Op de Hipt, F., Diekkrüger, B., Steup, G., Yira, Y., Hoffmann, T., Rode, M., 2017. Applying
953 SHETRAN in a Tropical West African Catchment (Dano, Burkina Faso)—Calibration, Val-
954 idation, Uncertainty Assessment. *Water* 9, 101. <https://doi.org/10.3390/w9020101>
- 955 Oudin, L., Hervieu, F., Michel, C., Perrin, C., Andréassian, V., Anctil, F., Loumagne, C., 2005.
956 Which potential evapotranspiration input for a lumped rainfall–runoff model? *Journal of*
957 *Hydrology* 303, 290–306. <https://doi.org/10.1016/j.jhydrol.2004.08.026>
- 958 Ouedraogo, I., Tigabu, M., Savadogo, P., Compaoré, H., Odén, P.C., Ouadba, J.M., 2010. Land
959 cover change and its relation with population dynamics in Burkina Faso, West Africa.
960 *Land Degradation & Development* 21, 453–462. <https://doi.org/10.1002/ldr.981>
- 961 Paeth, H., Capo-Chichi, A., Endlicher, W., 2008. Climate change and food security in tropical
962 West Africa – a dynamic-statistical modelling approach. *erdkunde* 62, 101–115.
963 <https://doi.org/10.3112/erdkunde.2008.02.01>
- 964 Pandey, A., Himanshu, S.K., Mishra, S.K., Singh, V.P., 2016. Physically based soil erosion and
965 sediment yield models revisited. *CATENA* 147, 595–620.
966 <https://doi.org/10.1016/j.catena.2016.08.002>
- 967 Paré, S., Söderberg, U., Sandewall, M., Ouadba, J.M., 2008. Land use analysis from spatial and
968 field data capture in southern Burkina Faso, West Africa. *Agriculture, Ecosystems & En-
969 vironment* 127, 277–285. <https://doi.org/10.1016/j.agee.2008.04.009>
- 970 Parkin, G., 1996. A three-dimensional variably-saturated subsurface modelling system for river
971 basins. (Phd thesis). Newcastle University, Newcastle upon Tyne, United Kingdom,
972 Newcastle upon Tyne <<https://theses.ncl.ac.uk/dspace/handle/10443/3161>>.
- 973 Pimentel, D., 2006. Soil Erosion: A Food and Environmental Threat. *Environment, Development
974 and Sustainability* 8, 119–137. <https://doi.org/10.1007/s10668-005-1262-8>
- 975 Roose, E., Kabore, V., Guenat, C., 1999. Zai Practice: A West African Traditional Rehabilitation
976 System for Semiarid Degraded Lands, a Case Study in Burkina Faso. *Arid Soil Research
977 and Rehabilitation* 13, 343–355. <https://doi.org/10.1080/089030699263230>
- 978 Roudier, P., Ducharne, A., Feyen, L., 2014. Climate change impacts on runoff in West Africa: a
979 review. *Hydrology and Earth System Sciences* 18, 2789–2801.
980 <https://doi.org/10.5194/hess-18-2789-2014>
- 981 Schmengler, A.C., 2010. Modeling soil erosion and reservoir sedimentation at hillslope and
982 catchment scale in semi-arid Burkina Faso (Phd thesis). Rheinische Friedrich-Wilhelms-
983 Universität Bonn, Bonn, <<http://hss.ulb.uni-bonn.de/2011/2483/2483.htm>>.
- 984 Schmengler, A.C., Vlek, P.L., 2015. Assessment of accumulation rates in small reservoirs by
985 core analysis, ¹³⁷Cs measurements and bathymetric mapping in Burkina Faso. *Earth
986 Surface Processes and Landforms* 40, 1951–1963. <https://doi.org/10.1002/esp.3772>
- 987 Shen, H.W., Julien, P.Y., 1993. Erosion and sediment transport, in: Maidment, D.R. (Ed.), *Hand-
988 book of Hydrology*. McGraw-Hill, New York.
- 989 Shuttleworth, W.J., 1993. Evaporation, in: Maidment, D.R. (Ed.), *Handbook of Hydrology*.
990 McGraw-Hill, New York.
- 991 Stephenne, N., Lambin, E.F., 2001. A dynamic simulation model of land-use changes in
992 Sudano-sahelian countries of Africa (SALU). *Agriculture, ecosystems & environment* 85,
993 145–161. [https://doi.org/10.1016/S0167-8809\(01\)00181-5](https://doi.org/10.1016/S0167-8809(01)00181-5)
- 994 The World Bank, 2017. Burkina Faso | Data [WWW Document]. Burkina Faso. URL
995 <http://data.worldbank.org/country/burkina-faso> (accessed 2.16.17).
- 996 Thiombiano, A., Kampmann, D., 2010. Biodiversity Atlas of West Africa, Volume II: Burkina Faso
997 (No. II). Ouagadougou & Frankfurt/Main.

998 Tripkovic, V., 2014. Quantifying and upscaling surface and subsurface runoff and nutrient flows
999 under climate variability (Phd thesis). Newcastle University, Newcastle upon Tyne,
1000 <<https://theses.ncl.ac.uk/dspace/handle/10443/2380>>.

1001 UNEP (United Nations Environmental Programme), 2012. Global Environment Outlook 4 (No. 4).
1002 UNEP, Valletta, Malta.

1003 Valentin, C., Rajot, J.-L., Mitja, D., 2004. Responses of soil crusting, runoff and erosion to fallow-
1004 ing in the sub-humid and semi-arid regions of West Africa. *Agriculture, Ecosystems &*
1005 *Environment* 104, 287–302. <https://doi.org/10.1016/j.agee.2004.01.035>

1006 Wagner, P.D., Kumar, S., Schneider, K., 2013. An assessment of land use change impacts on
1007 the water resources of the Mula and Mutha Rivers catchment upstream of Pune, India.
1008 *Hydrology and Earth System Sciences* 17, 2233–2246.

1009 Wicks, J.M., 1988. Physically-based mathematical modelling of catchment sediment yield (Phd
1010 thesis). Newcastle University, Newcastle upon Tyne
1011 <<https://theses.ncl.ac.uk/dspace/handle/10443/152>>.

1012 Wicks, J.M., Bathurst, J.C., 1996. SHESED: a physically based, distributed erosion and sedi-
1013 ment yield component for the SHE hydrological modelling system. *Journal of Hydrology*
1014 175, 213–238. [https://doi.org/10.1016/S0022-1694\(96\)80012-6](https://doi.org/10.1016/S0022-1694(96)80012-6)

1015 Wilson, C.O., Weng, Q., 2011. Simulating the impacts of future land use and climate changes on
1016 surface water quality in the Des Plaines River watershed, Chicago Metropolitan Statisti-
1017 cal Area, Illinois. *Science of The Total Environment* 409, 4387–4405.
1018 <https://doi.org/10.1016/j.scitotenv.2011.07.001>

1019 Yira, Y., 2016. Modelling Climate and Land Use Change Impacts on Water Resources in the
1020 Dano Catchment (Burkina Faso, West Africa) (Phd thesis). Rheinische Friedrich-
1021 Wilhelms-Universität Bonn, Bonn, <<http://hss.ulb.uni-bonn.de/2017/4583/4583.htm>>.

1022 Yira, Y., Diekkrüger, B., Steup, G., Bossa, A.Y., 2017. Impact of climate change on hydrological
1023 conditions in a tropical West African catchment using an ensemble of climate simula-
1024 tions. *Hydrology and Earth System Sciences* 21, 2143–2161.
1025 <https://doi.org/10.5194/hess-21-2143-2017>

1026 Yira, Y., Diekkrüger, B., Steup, G., Bossa, A.Y., 2016. Modeling land use change impacts on
1027 water resources in a tropical West African catchment (Dano, Burkina Faso). *Journal of*
1028 *Hydrology* 537, 187–199. <https://doi.org/10.1016/j.jhydrol.2016.03.052>

1029 Zhang, R., 2015. Integrated modelling for evaluation of climate change impacts on agricultural
1030 dominated basin (Phd thesis). University Evora, Evora
1031 <<https://dspace.uevora.pt/rdpc/handle/10174/13270>>.

1032 Zhang, X.-C., Nearing, M.A., Garbrecht, J.D., Steiner, J.L., 2004. Downscaling Monthly Fore-
1033 casts to Simulate Impacts of Climate Change on Soil Erosion and Wheat Production. *Soil*
1034 *Science Society of America Journal* 68, 1376. <https://doi.org/10.2136/sssaj2004.1376>

1035

Table 1: Initial LULC classes as given by Landmann et al. (2007) and Forkour (2014) and reclassified classes used in this study

Initial LULC classes	Proportional area [%] in year							Reclassified LULC classes
	1990	2000	2007	2013	2019	2025	2030	
Regularly flooded, woody, closed to open	1.03	29.2	-	-	-	-	-	Tree and shrub savannah
Broadleaved forest, closed, evergreen (>=65%)	1.77	-	-	-	-	-	-	Tree and shrub savannah
Woodland, closed (40 – 65%)	5.22	-	-	-	-	-	-	Tree and shrub savannah
Woodland closed/forest closed	59.3	-	8.80	-	-	-	-	Tree and shrub savannah
Reg. flooded, high confidence	1.16	-	-	-	-	-	-	Tree and shrub savannah
Burned area	4.03	2.64	-	-	-	-	-	Cropland
Bare soil scattered vegetation	1.00	-	-	-	-	-	-	Urban area
Regularly flooded wetland	0.84	-	-	-	-	-	-	Tree and shrub savannah
Herbaceous crops	8.28	-	-	-	-	-	-	Cropland
Herbaceous vegetation, closed (>=65%)	17.28	-	-	-	-	-	-	Tree and shrub savannah
Forest	-	3.45	15.5	-	-	-	-	Tree and shrub savannah
Grassland	-	35.1	46.7	-	-	-	-	Tree and shrub savannah
Cropland	-	16.1	20.4	36.3	42.3	48.3	54.5	Cropland
Wetland	-	13.2	1.52	-	-	-	-	Tree and shrub savannah
Urban area	-	0.16	6.54	5.19	7.19	9.19	11.1	Urban area
Water	-	-	0.42	0.39	0.39	0.39	0.39	Water
Natural/-semi-natural Vegetation	-	-	-	58.1	50.0	42.0	33.9	Tree and shrub savannah

Table 2: Applied datasets and required inputs for SHETRAN

Data set	Spatiotemporal resolution / scale	Source	Derived parameters
Topography	90 m	SRTM (Jarvis et al., 2008)	
Soil	1:25 000	Soil survey	Soil hydrological parameters (α , n ¹⁾ , K_{sat} ²⁾ , θ_{sat} ³⁾ , θ_{res} ⁴⁾) texture etc.
Land use maps	5 to 250 m	Forkuor (2014), Landmann et al. (2007)	Land use type distribution
Land use characteristic		Literature	LAI ⁵⁾ , Strickler coefficient, ETa/ETp ratio ⁶⁾
Meteorological data	Hourly, Daily	Instrumentation WASCAL, DGM ⁷⁾ , CORDEX ⁸⁾	Rainfall, temperature, humidity, solar radiation, wind speed
Discharge	Hourly	Instrumentation WASCAL	Discharge
Erosion	Hourly, Event	Instrumentation WASCAL	Suspended sediment load, soil erosion rate

¹⁾ α and n are van Genuchten empirical parameters, ²⁾ K_{sat} refers to the saturated hydraulic conductivity, ³⁾ θ_{sat} to the saturated water content, ⁴⁾ θ_{res} to the residual water content, ⁵⁾ LAI to the leaf area index and ⁶⁾ ETp/ETa ratio to the ratio of potential evapotranspiration to actual evapotranspiration, ⁷⁾Direction Général de la Météorologie du Burkina, ⁸⁾Coordinated Regional climate Downscaling Experiment project

Table 3: Soil, land use and erosion parameters in SHETRAN (NV: natural vegetation (mainly savannah), CR: crop land, SM: settlement)

Parameter	Description	Unit	Parameter range	Source
Hydrology				
ETa/ETp at field capacity (varies with land use type)	Ratio of actual evapotranspiration to potential evapotranspiration at field capacity	-	CR ¹⁾ : 0.5 NV ²⁾ : 0.6 SM ³⁾ : 0.1	Shuttleworth (1993)
KSTR (varies with land use type)	Strickler roughness coefficient	m ^{1/3} s ⁻¹	CR: 1.4 NV: 0.6 SM: 6.0	Mohamoud (1992), Shen and Julien (1993)
Soil erosion				
k_r (soil invariant)	Overland flow soil erodibility	kg m ⁻² s ⁻¹	7.5×10 ⁻¹¹	Calibration
k_r (varies with texture)	Raindrop soil erodibility coefficient	J ⁻¹	0.19 – 7.9	Adams and Elliott (2006), Birkinshaw et al. (2010a), de Figueiredo and Bathurst (2007), Elliott et al. (2011), Lukey et al. (2000, 1995), Norouzi Banis et al. (2004), Wicks and Bathurst (1996)
BKB (soil invariant)	Channel bank erodibility coefficient	kg m ⁻² s ⁻¹	1×10 ⁻⁶ – 3×10 ⁻⁶	Calibration
DLSMAX	Threshold depth of loose sediment	mm	1×10 ⁻⁶ – 9.9×10 ⁻⁶	Calibration

Table 4: LULC simulations, model periods and applied land use maps.

Data	Simulation name	Simulation period							
		Warm-up period	Evaluation period						
		1990 – 1996	1997 – 2005	-	-	-	-	-	
Observed climate and LULC maps	M1_1990	LULC_1990	LULC_1990	-	-	-	-	-	
	M2_2000	LULC_1990	LULC_2000	-	-	-	-	-	
	M3_2007	LULC_1990	LULC_2007	-	-	-	-	-	
	M4_2013	LULC_1990	LULC_2013	-	-	-	-	-	
		Warm-up period	Evaluation period						
		1990 – 1996	1997 – 2003	2004 – 2010	2011 – 2015	-	-	-	
	M5_90/13	LULC_1990	LULC_2000	LULC_2007	LULC_2013	-	-	-	
Data	Simulation name	Warm-up period	Evaluation period						
		1990 – 1996	1997 – 2005	-	-	-	-	-	
Observed climate and modeled LULC maps	M6_2019	LULC_1990	LULC_2019	-	-	-	-	-	
	M7_2025	LULC_1990	LULC_2025	-	-	-	-	-	
	M8_2030	LULC_1990	LULC_2030	-	-	-	-	-	
Data	Simulation name	Warm-up period	Evaluation period						
		1990 - 1996	1997 – 2005	2006 – 2010	2011 – 2016	2017-2022	2023-2027	2028-2032	
Modeled climate and observed LULC map	M9_1990_RCP4.5	LULC_1990	LULC_1990						
	M10_1990_RCP8.5	LULC_1990	LULC_1990						
Modeled climate and modeled LULC maps	M11_90/30_RCP4.5	LULC_1990	LULC_2000	LULC_2007	LULC_2013	LULC_2019	LULC_2025	LULC_2030	
	M12_90/30_RCP8.5	LULC_1990	LULC_2000	LULC_2007	LULC_2013	LULC_2019	LULC_2025	LULC_2030	
Data	Simulation name	Warm-up period	Evaluation period						
		1984 - 1997	1998 - 2005	-	-	-	-	-	
Past modeled climate and observed LULC maps	M13_1990	LULC_1990	LULC_1990	-	-	-	-	-	
	M14_2000	LULC_1990	LULC_2000	-	-	-	-	-	
	M15_2007	LULC_1990	LULC_2007	-	-	-	-	-	
	M16_2013	LULC_1990	LULC_2013	-	-	-	-	-	
		Simulation name	Warm-up period	Evaluation period					
			1984 - 1989	1990 - 1997	1998 - 2005	-	-	-	-
	M17_90/13	LULC_1990	LULC_1990	LULC_2000	-	-	-	-	

Table 5: Average annual water balance and specific suspended sediment yield of simulation driven by observed climate. The evaluation period from 1997 – 2005 is marked by *, the evaluation period from 1997 – 2015 is marked by **

Simulation	M1_1990	M2_2000	M3_2007	M4_2013	M5_90/13	M6_2019	M7_2025	M8_2030
Mean annual rainfall [mm]	877*/903**	877*/903**	877*/903**	877*/903**	903**	877*/903**	877*/903**	877*/903**
Mean annual ETp [mm]	1826*/1809*	1826*/1809*	1826*/1809*	1826*/1809*	1809**	1826*/1809*	1826*/1809*	1826*/1809*
Mean annual ETa [mm]	846*/844**	840*/839**	821*/820**	818*/820**	827**	812*/822**	797*/802**	784*/786**
Mean annual water yield [mm]	39.4*/59.4**	40.8*/61.7**	57.7*/81.2**	52.7*	71.4**	60*/86.7**	67.1*/95.5**	75.5*/105**
Mean annual specific suspended sediment yield [t/ha]	0.021*/0.0317**	0.021*/0.0312**	0.032*/0.0449**	0.031*/0.0445**	0.0395**	0.038*/0.0531**	0.043*/0.0599**	0.051*/0.0684**

Table 6: Average annual water balance and specific suspended sediment yield. Annual means of the modeled past (1990 – 2005)^{a)} and the modeled scenarios (2006 – 2032)^{b)} are indicated for simulations M9 – M12. The evaluation period from 1998 – 2005 for M13-M17 is marked by *, the evaluation period from 1998 – 2015 is marked by **

Simulation	M9_1990_RCP4.5	M10_1990_RCP8.5	M11_90/30_RCP4.5	M12_90/30_RCP8.5	M13_1990	M14_2000	M15_2007	M16_2013	M17_90/2005
Mean annual rainfall [mm]	951 ^{a)} – 1026 ^{b)}	951 ^{a)} – 1002 ^{b)}	951 ^{a)} – 1026 ^{b)}	951 ^{a)} – 1002 ^{b)}	997*/951**	997*/951**	997*/951**	997*/951**	951**
Mean annual ETp [mm]	1578 ^{a)} – 1653 ^{b)}	1578 ^{a)} – 1674 ^{b)}	1578 ^{a)} – 1653 ^{b)}	1578 ^{a)} – 1674 ^{b)}	1616*/157 8**	1616*/157 8**	1616*/157 8**	1616*/157 8**	1578**
Mean annual ETa [mm]	775 ^{a)} – 799 ^{b)}	775 ^{a)} – 801 ^{b)}	768 ^{a)} – 756 ^{b)}	768 ^{a)} – 761 ^{b)}	798*/784**	794*/780**	776*/763**	771*/758**	781**
Mean annual water yield [mm]	154 ^{a)} – 226 ^{b)}	154 ^{a)} – 192 ^{b)}	152 ^{a)} – 264 ^{b)}	152 ^{a)} – 229 ^{b)}	170.6*/157 .9**	176.5*/164 .7**	194.3*/182 .3**	198.9*/187 .5**	160.4**
Mean annual specific suspended sediment yield [t/ha]	0.084 ^{a)} – 0.13 ^{b)}	0.084 ^{a)} – 0.11 ^{b)}	0.082 ^{a)} – 0.15 ^{b)}	0.082 ^{a)} – 0.13 ^{b)}	0.097*/0.0 9**	0.099*/0.1 02**	0.112*/0.1 1**	0.120*/0.0 87**	0.087**

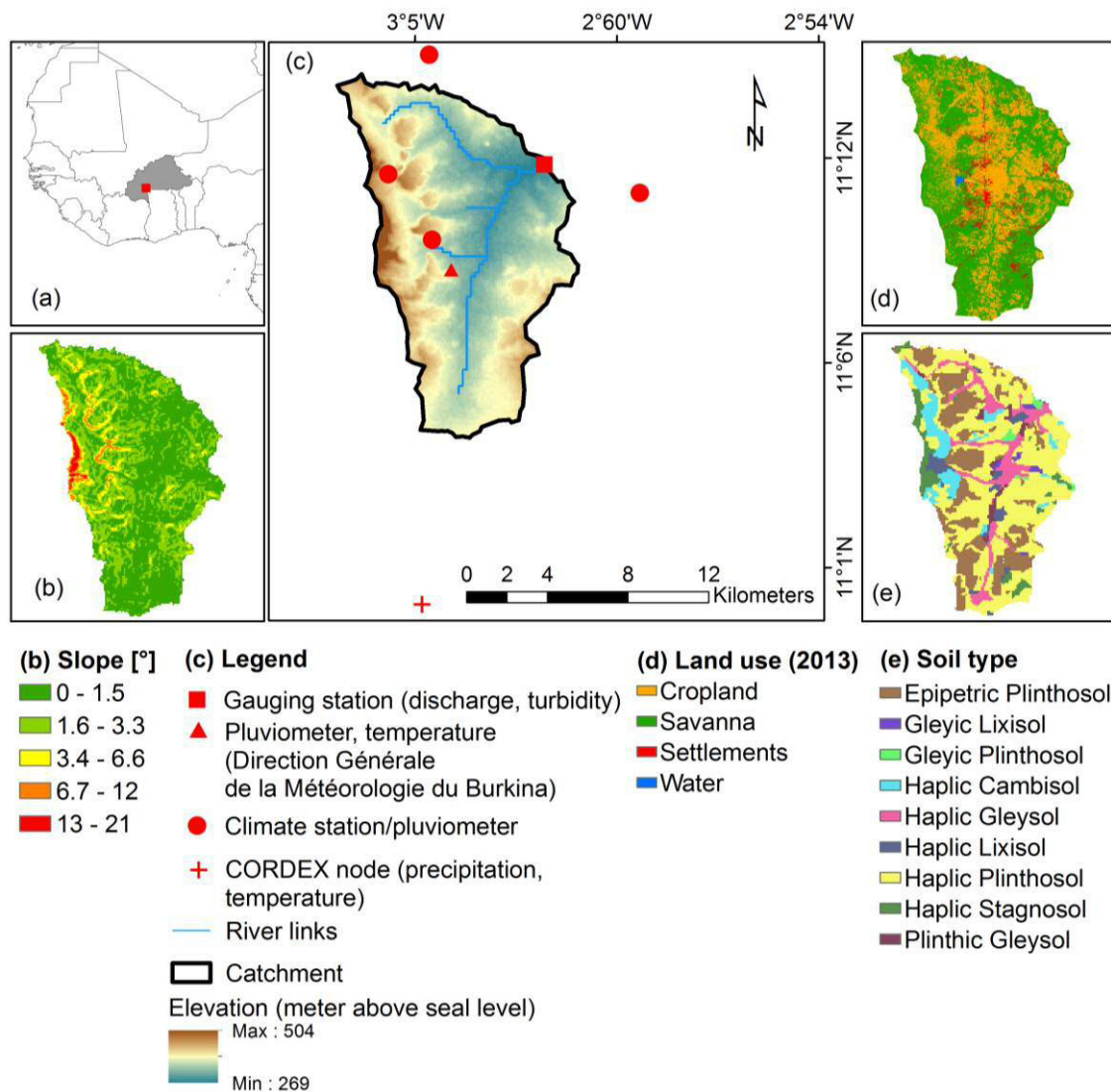


Figure 1: Location map of the Dano catchment: (a) location of the catchment and Burkina Faso in West Africa, (b) slope of the catchment, (c) model catchment, (d) land use map (Forkuor, 2014), (e) soil map (data base: soil survey done by Ozias Hounkpatin, Soil Science of Institute of Crop Science and Resource Conservation, University Bonn). DGM refers to the Direction Générale de la Météorologie du Burkina.

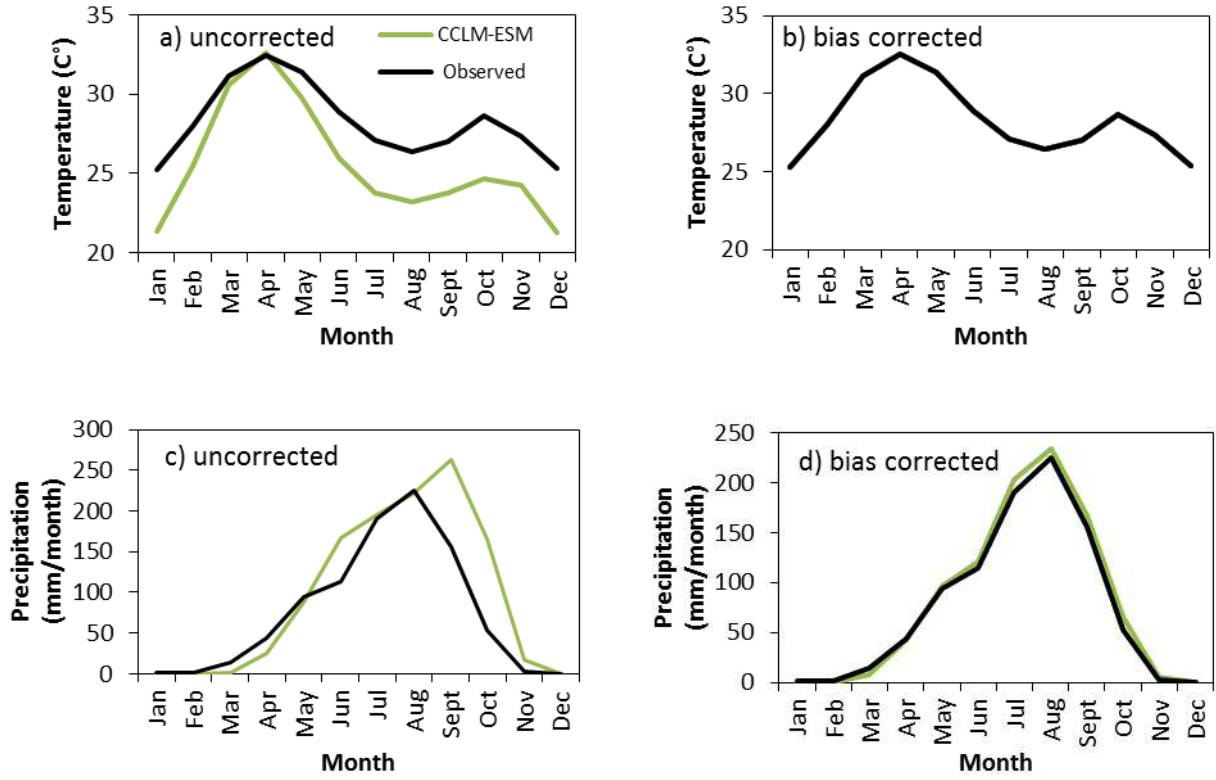


Figure 2: Uncorrected and bias corrected temperature (a, b) and precipitation (c, d).

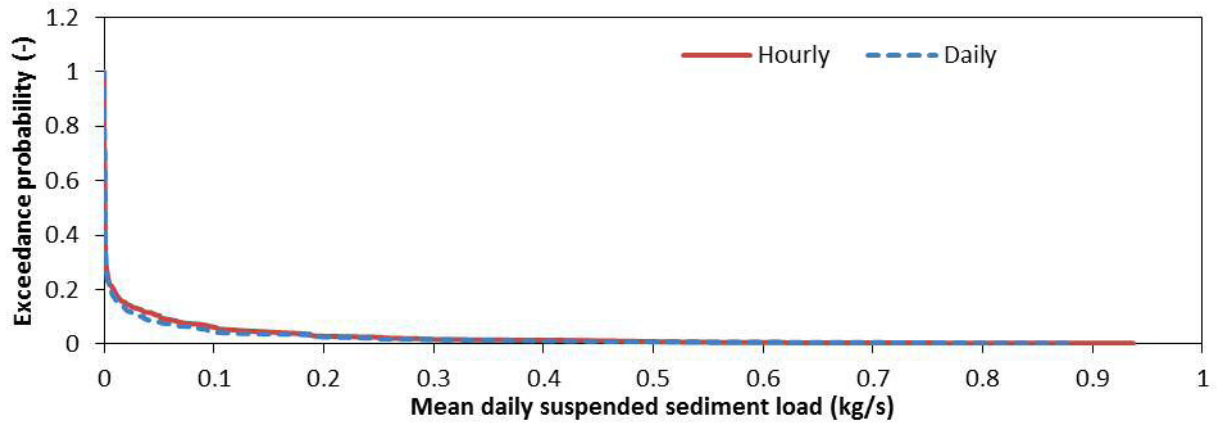


Figure 3: Exceedance probability of hourly and daily suspended sediment load

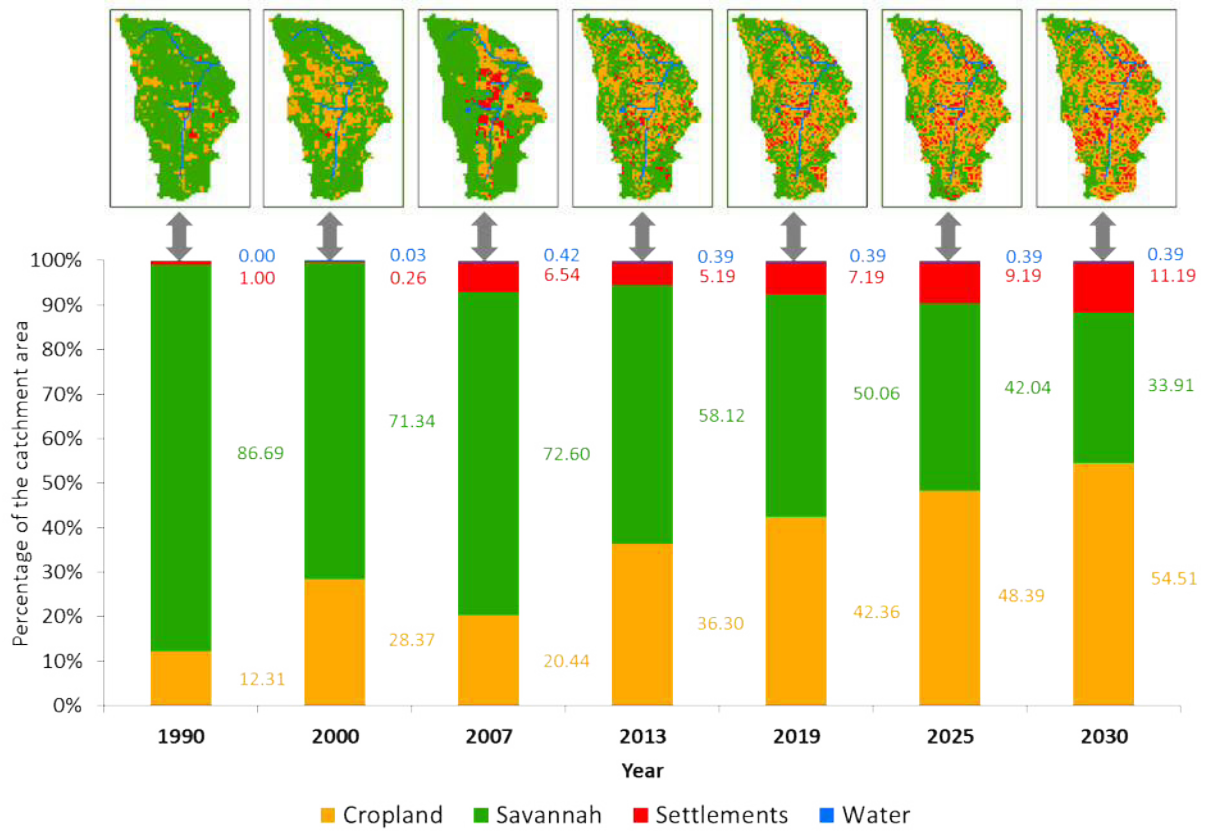


Figure 4: Observed (1990 – 2013) and modeled (2019 – 2030) LULC maps and the corresponding relative proportion of each land use.

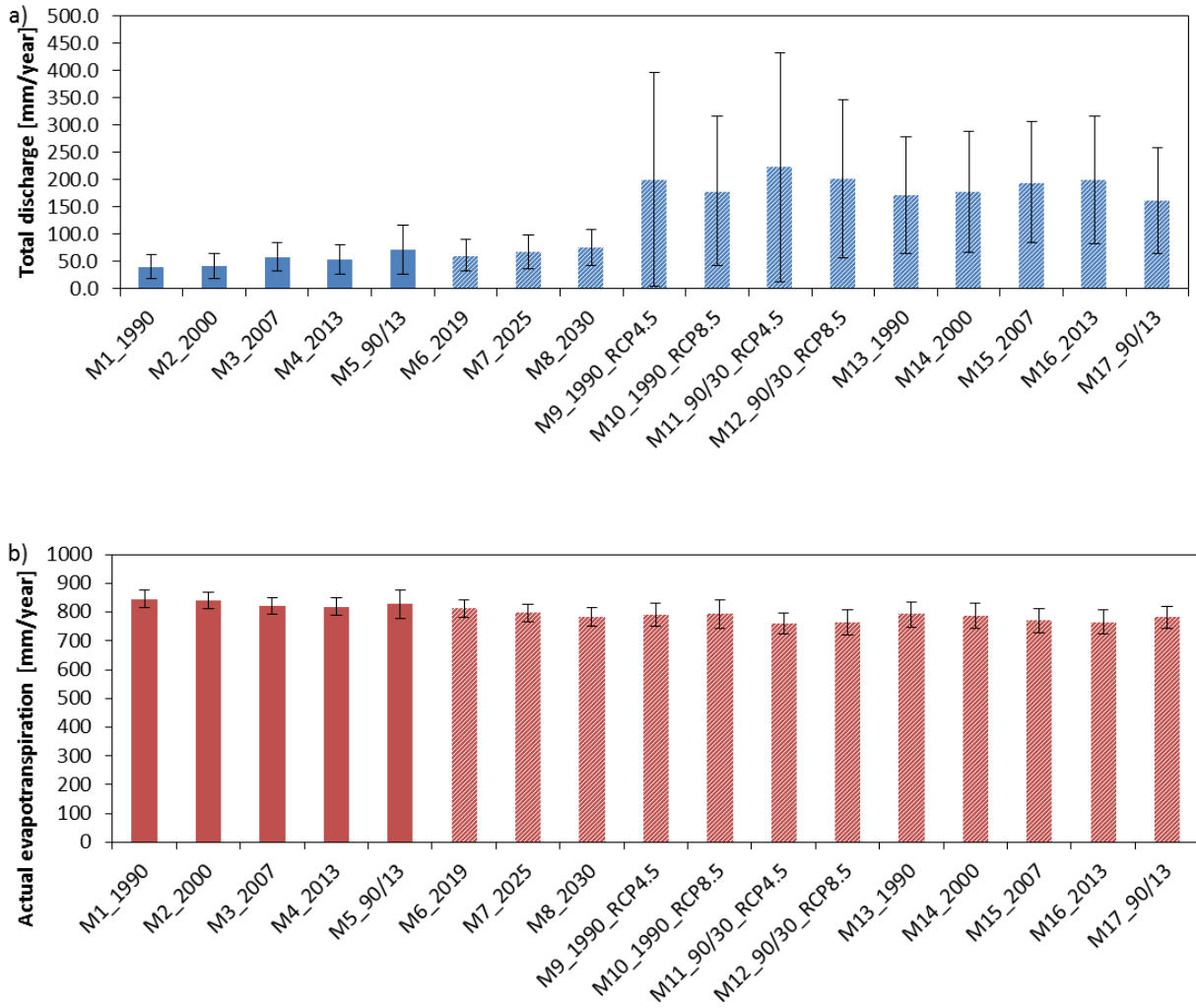


Figure 5: a) Mean annual total water yield for M1_1990 – M12_90/30_RCP8.5 and b) mean annual actual evapotranspiration for simulations M1_1990 – M12_90/30_RCP8.5. Error bars indicate the standard deviation calculated based on annual sums. Dashed bars indicate the use of modeled LULC and/or climate. See Tab. 4 and the text for explanation of the different scenarios

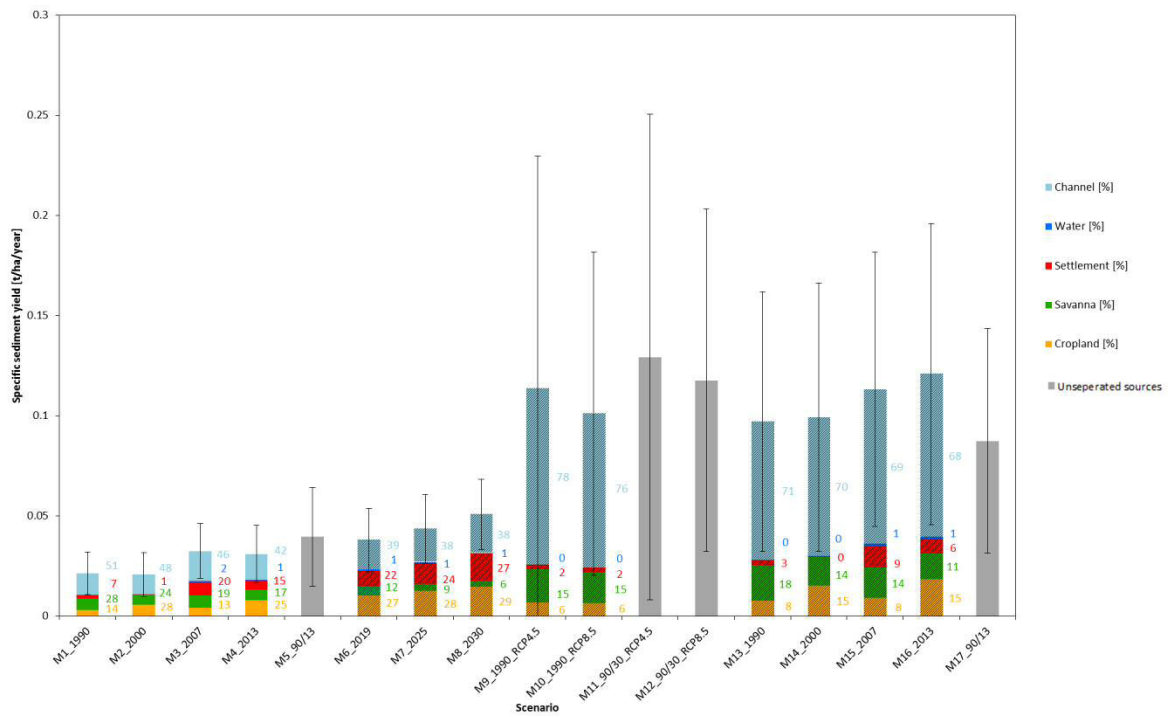


Figure 6: Mean annual specific suspended sediment yield for the simulations M1_1990 – M12_90/30_RCP8.5. The contribution of each source is given in % for all simulations except for the continuous simulations (M5, M11, M12, M17). Error bars indicate the standard deviation calculated based on annual sums. Dashed bars indicate the use of modeled LULC maps and/or modeled climate data.

